UCD

College of Engineering

University of California, Davis

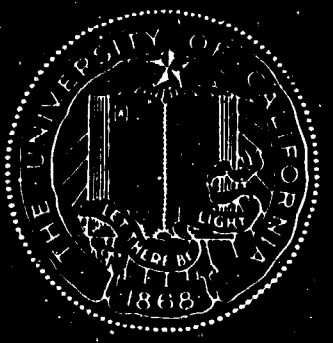

FINAL SCIENTIFIC REPORT

"Fundamental Investigations of Failure During Superplastic Forming Process"

by

Amiya K. Mukherjee

Division of Materials Science and Engineering

SECURITY CLASSIFICATION OF THIS PAGE (When Data Entered)

REPORT DOCUMENTATION PAGE

READ INSTRUCTIONS BEFORE COMPLETING FORM

1. REPORT NUMBER: AFOSR-TR- 86-0482
2. GOVT ACCESSION NO: AD-A169740
3. RECIPIENT'S CATALOG NUMBER:

4. TITLE (and Subtitle): Fundamental Investigations of Failure During Superplastic Forming Process
5. TYPE OF REPORT & PERIOD COVERED: 2/1/82 to 1/31/86, FINAL
6. PERFORMING ORG. REPORT NUMBER:

7. AUTHOR(s): A. K. Mukherjee
8. CONTRACT OR GRANT NUMBER(s): AFOSR-82-0081

9. PERFORMING ORGANIZATION NAME AND ADDRESS:
Div. of Materials Science and Engineering
Dept. of Mechanical Engineering
University of California, Davis, CA 95616
10. PROGRAM ELEMENT, PROJECT, TASK AREA & WORK UNIT NUMBERS:
6-1102F
2306/A1

11. CONTROLLING OFFICE NAME AND ADDRESS:
Dr. Alan Rosenstein
AFOSR/NE, Building 410
Bolling Air Force Base, D.C. 20332-6448
12. REPORT DATE: April 1986
13. NUMBER OF PAGES: 96

14. MONITORING AGENCY NAME & ADDRESS (if different from Controlling Office): nm
15. SECURITY CLASS. (of this report): Unclassified
15a. DECLASSIFICATION/DOWNGRADING SCHEDULE:

16. DISTRIBUTION STATEMENT (of this Report)

Unlimited

17. DISTRIBUTION STATEMENT (of the abstract entered in Block 20, if different from Report)

Unlimited

18. SUPPLEMENTARY NOTES

To be published in Materials Science and Engineering and Acta Metallurgica

19. KEY WORDS (Continue on reverse side if necessary and identify by block number)

Superplasticity, constitutive equation, mechanical behavior, deformation mechanisms, cavitation phenomenon.

20. ABSTRACT (Continue on reverse side if necessary and identify by block number)

The superplastic properties of Ti-6Al-4V, Ti-6Al-4V-2Ni and 7475-T6 aluminum alloys were investigated with special emphasis on correlation between mechanical behavior and microstructure. The rate parameters for constitutive equation for superplasticity in these alloys were established. The variation in the values of these parameters from the prediction of steady-state models was explained in the context of microstructural evolution. The effect of hydrostatic gas pressure in minimizing cavitation in the aluminum alloy was emphasized.

DD FORM 1 JAN 73 1473

U/C

SECURITY CLASSIFICATION OF THIS PAGE (When Data Entered)

FINAL SCIENTIFIC REPORT

GRANT - AFOSR-82-0081

Period 2/1/82 to 1/31/86

Fundamental Investigations of Failure During Superplastic Forming Process

by

Professor Amiya K. Mukherjee

Division of Materials Science and Engineering

Department of Mechanical Engineering

University of California

Davis, California 95616

Dr. Alan Rosenstein

Air Force Office of Scientific Research

AFOSR/NE

Building 410

Bolling Air Force Base

D.C. 20332-6448

April 1986

CONTENTS

ABSTRACT

The experimental work on both the base alpha-beta alloy (Ti-6Al-4V) and the Ni-modified alloy (Ti-6Al-4V-2Ni) showed that there is significant microstructural evolution during superplastic deformation. These structural evolutions affect the parameters for the constitutive equation for superplasticity. Contrary to model prediction, the strain rate sensitivity is found to be a function of temperature, in a way that exactly parallels the dependence of beta-volume fraction on temperature. An empirical equation has been proposed to characterize the non-steady state microstructure in terms of the dependence of strain hardening coefficient on temperature and strain rate. The maximum attainable ductility in this alloy is associated with a dynamic balance between strain hardening (due to grain growth) and strain softening (due to in situ grain refinement).

The 7475-T6 aluminum alloy (heat B) undergoes significant level of strain hardening due to increase in dislocation density as a function of strain. The grains do not remain equiaxed (which is contrary to most supposition of superplasticity). One does not observe a true steady-state in the microstructure during superplastic deformation. The activation energy of deformation is equal to that for volume diffusion, possibly due to the necessity of the dislocations to climb over the Cr-rich particles. The alloy cavitates extensively due to decohesion of the intermetallic particle/grain boundary interface. Superplastic ductility in this alloy is increased substantially by superimposing hydrostatic argon gas pressure during deformation. The most remarkable fact is that this extraordinary ductility can be achieved by virtually eliminating internal grain boundary cavitation, at a critical argon gas pressure. Ongoing experiments are expected to shed light on whether the effect of such gas pressure is to reduce the nucleation rate, growth rate or both, for the cavitation phenomenon.

SECTION 1

INTRODUCTION

The scientific aspect of this research program is designed to clarify the mechanical and microstructural properties in superplasticity. There are several specific areas of emphasis:

(a) Substructural investigation with critical attention paid to the structural modification induced by superplastic flow.

(b) Delineation of ranges of operation of the superplastic process in terms of temperature, strain rate and stress.

(c) Determination of the parameters of the constitutive equation for superplastic flow; the dependence of these parameters on structural evolution, if present.

(d) Investigation on the cavitation characteristics of the aluminum alloy and preliminary exploration of the effect of superimposed hydrostatic gas pressure in minimizing such cavitation.

The three prime requirements for the manifestation of micrograin superplasticity are (a) a fine (less than 15μm) and equiaxed grain size that is reasonably stable during deformation, (b) the temperature must be more than about half of the melting point of the matrix in absolute degrees and (c) a strain rate that is typically not too high (less than 10^{-2} s^{-1}) or too low (more than 10^{-6} s^{-1}). Most superplastic materials are either dual-phase alloys (often eutectics or eutectoids) or they have quasi single phase microstructure where there are intermetallic particles at the grain

boundaries. Such materials satisfy the condition of some degree of stability of the microstructure (i.e., criterion "a") because the strain enhanced grain growth is minimized by the chemical dissimilarity of the two phases in the dual phase microstructure or by pinning of the grain boundary by particles in the quasi single phase alloys. The second criterion essentially refers to the fact that solid state diffusion controlled processes are operative in superplasticity and as such superplasticity is a generic cousin of all other elevated temperature creep mechanisms. The third criterion essentially assures that the strain rate sensitivity parameter has a value large enough to promote the stability of external necks. For large values of this parameter, the strain rate of a material near a neck and the rest of the specimen are nearly equal. This minimizes the tendency for localized necking (in tensile tests) and hence premature failure and thus, in the absence of internal cavitation, leads to large overall total elongation.

The report discusses the results obtained from the superplastic deformation of three alloys:

(i) Ti-6Al-4V

(ii) Ti-6Al-4V-2Ni

(iii) 7475-T6 aluminum alloy, thermomechanically processed for fine grain size.

The first two alloys have dual-phase microstructure of alpha and beta. The third alloy has a matrix of essentially single phase (solid solution) where the grain boundaries are pinned by Cr-rich particles.

(A) Titanium Alloys

Superplastic deformation of titanium alloys is now a viable metal forming process in the aerospace industries. Many such airframe components are

fabricated using the Ti-6Al-4V alloy. In fact, the superplastic forming and diffusion bonding technology is based on this alloy.

A significant amount of research has been devoted to the base Ti-6Al-4V alloy. However, the microstructure of such alloy system cannot, in general, be adequately characterized by a single parameter such as the grain size. In the two phase alpha-beta Ti-6Al-4V alloy, other microstructural parameters, in addition to grain size, have been found to affect superplasticity. Metallurgical variables in titanium alloy system, such as volume fractions of the two phases, grain size distribution, grain growth and grain refinement kinetics and difference in the diffusivities of the two phases may also influence the superplastic behavior. In addition, the alloy composition could be a significant variable, having pronounced effect on parameters such as phase ratio and diffusivity.

The experimental results indicate that, unlike many other superplastic alloys, the microstructure in superplastic titanium alloys does not remain stable during deformation. Recent work on grain size distribution effect suggests that the presence of small fractions of large grains distributed among fine grains can have a strong effect on the flow characteristics at superplastic forming temperatures. Similar effect can be produced by the α/β phase ratio of the microstructure. It has been determined that all-alpha or all-beta Ti alloys exhibit very limited ductility at high temperatures. On the other hand, it has been shown that α-β alloys offer the maximum degree of superplasticity, with the beta-phase (softer) having the highest diffusivity, and, as such being instrumental in the diffusion assisted mechanisms necessary for superplastic flow. However, the grain coarsening rate of the β-phase is such that it is necessary to have a sufficient amount of the hard α-phase to

restrict the growth of β-phase. Otherwise, the grain size becomes rapidly too large for effective superplastic flow. With appropriate α/β proportion, the α-phase serves the function of restricting the phase growth of beta and thus a two-phase alloy can retain the relatively fine grain size long enough for superplastic deformation to occur.

Ni Modified Ti-6Al-4V Alloy

The Ti-6Al-4V alloy displays optimum superplastic properties near 927°C, the temperature frequently used for SPF of full scale components with this alloy. However, lower superplastic forming (SPF) temperatures would be desirable to reduce oxidation problems, to shorten forming cycle times, and to reduce die cost. Investigations for developing new Ti-based alloys with lower SPF temperatures have been prompted by a better understanding of semi-quantitative features of the superplastic characteristics of Ti alloys. It has been established that alloy modifications to lower the optimum SPF temperature of the Ti-6Al-4V base alloy must alter two characteristics of the material:

1. A large volume fraction of the β-phase appears essential to SPD of titanium alloys. Some evidence suggests that obtaining equal volume fractions of the two phases in a duplex alloy produces optimum superplastic properties. Thus, the alloy modification must stabilize the β-phase so as to increase the volume fraction of this phase at temperatures below the conventional SPF temperature of the base alloy.

2. Creep processes such as grain boundary sliding (GBS) and diffusion are essential to SPD. In the base alloy, Ti-6Al-4V, these creep processes proceed too slowly at temperatures below 927°C to contribute substantially to the total strain. Alloy additions with high diffusivity can accelerate creep

rates, allowing the creep process essential to SPD to proceed at reasonable rates below the conventional SPF temperatures for the base alloy.

The work of Wert and Paton (North American Rockwell Science Center) as well as that by Leader, Neal and Hammond (University of Leeds) pointed out that the alloying element Ni appears to have the best combination of conditions for β-transus depression, along with the highest diffusivity in β-Ti phase. The composition of Ti-6Al-4V-2Ni was chosen for this investigation because some preliminary base results were already available on this alloy.

The investigation on the superplastic deformation behavior of the Ti-6Al-4V base alloy as well as the Ni was conducted with two basic purposes in mind. From a practical point of view, our interest is the characterization of the flow behavior in this alloy as it correlates with microstructural observations. The aim is to determine the high temperature deformation parameters for optimum superplastic forming. From a scientific point of view, our main objective is understanding the fundamentals of superplastic deformation phenomena. Relatively more emphasis has been given to this last objective. In particular, the scientific aspects of the investigation is focussed on the following objectives:

(a) Better theoretical models for SPD, particularly for two-phase alloys, taking into account the effect of each phase as well as interphase-related phenomena on the superplastic flow.

(b) A better formulation for the kinetics of microstructural evolution, especially that for phase growth and/or phase refinement, as well as interphase accommodation process occurring during SPD.

Significant Results for Ti-Alloy System

The results of the investigation on the Ti-6Al-4V alloy are described in Section 2 of this report under the title "Strain Rate Sensitivity and Its Dependence or Microstructural Evolution During Superplastic Deformation." It is the outcome of the dissertation work of Michael Meier. The results of the investigation on the Ni-modified alloy is described in Section 3, under the heading "Correlation Between Mechanical Properties and Microstructure In A Ni-modifed Superplastic Ti-6Al-4V Alloy." This section is a synopsis of the dissertation work of Benjamin Hidalgo-Prada.

In this subsection we will summarize only the major experimental results and conclusions.

SUMMARY OF RESULTS

Ti-6Al-4V Alloy

1. The majority of the theoretical models for superplasticity suggest that the stress-sensitivity of the strain rate, n, has a value equal to about 2 and more importantly it is not a function of temperature (at constant strain rate). We observed that the invariance of n with temperature does not hold true for this alloy. The parameter n varies with temperature in a manner that strongly suggests that the role of the volume fraction of phases is directly responsible for the strain rate sensitivity of this alloy. However, the exact manner in which n varies with temperature depends on the test used to measure it (see section 2). These differences reflect on the true nature of n and has important implications on the significance attached to it.

2. The activation energy on the other hand is independent of strain rate and temperature. However, the values obtained are too high to be correlated with self-diffusion.

3. The grain size densitivity is equal to one, which is lower than that normally reported for superplasticity. Microstructural evolution during superplastic deformation is dominated by recrystallization, but also includes redistribution of phases and certain amount of grain growth. These observations, coupled with the correlation between volume fraction and the stress exponent requires that any realistic model regarding the mechanisms for superplastic deformation in such alloy must incorporate the different roles of each phase present in the alloy.

4. The strain hardening coefficient (an important parameter for superplastic forming) in this alloy is found to be dependent on temperature and strain rate. An empirical equation has been proposed (Equation 4, Section 2 of this report) to describe the linear portion of this dependence (Fig. 7, Section 2). Although the equation is empirical, it is a first attempt to characterize nonsteady state superplastic deformation. It fits the data reasonably well and covers a wide range of temperature and strain rates. It is useful in predicting the extent of strain hardening or softening behavior and in determining the optimum limits for uniform strain (i.e., before onset of neck-related instability).

Ni-Modified Ti-6Al-4V Alloy (Summary of Results)

1. There is significant microstructural evolution in this alloy during S.P.D. Both the strain hardening index, h, and the strain rate sensitivity (SRS) will control the ductility that the material may experience before the onset of plastic instability.

2. The investigation emphasizes the distinction between apparent strain rate sensitivity (ASRS) which is what is usually measured experimentally and the true strain rate sensitivity (SRS), that is related to the theoretical

constitutive expression for superplastic flow. The two are related by the Herriot-Baudelet-Jonas correlation by incorporating the changes in the phase size and distribution as a function of strain.

3. Maximum elongation to fracture in the Ni-modified alloy at a given test temperature, is proportional to apparent strain rate sensitivity (ASRS). However, this correlation is not necessarily maintained when comparing data at various temperatures, due to combined effects of phase proportion and microstructural evolution. Only at intermediate strain rates ($\sim 10^{-4}$ s^{-1}) and at SPF forming temperature of 815°C for which the volume fraction of α and β phases are equal, does the maximum value of ASRS correlate with maximum elongation to fracture.

4. It was found that the effect of microstructural changes occuring during SPD produced strain hardening and strain softening. Metallographic evidence is presented to show that the observed strain hardening is due to deformation-enhanced grain growth of both alpha and beta phases. The strain softening was primarily due to grain size refinement. Maximum attainable superplastic ductility was found to be associated with a dynamic balance between strain hardening and softening.

5. It appears that the rate controlling deformation process is that of interphase accomodation in agreement with the Spingarn-Nix model for deformation in two phase material by diffusion creep.

(B) Superplastic Aluminum Alloy

The first type of the new generation of superplastic aluminum alloys (these are essentially single phase) relies on the presence of fine precipitates at the grain boundaries in order to maintain the fine grain size. The present investigation on 7475-Al and similar alloys refers to the

alloys of this type. Quite extensive superplastic formability has been demonstrated in fine grain processed 7475-Al alloy. Practical and theoretical studies have shown substantial advantages for fabrication of aerospace and other structural components by superplastic forming compared with conventionally fabricated components. There are the benefits of near-net shape forming, saving in materials and machining costs, often an isotropic mechanical properties (primarily due to grain rotation during superplasticity) and a fairly good surface finish.

However, one undesirable characteristic of the fine grained 7475-Al is the tendency to cavitate in an intergranular fashion during superplastic forming. This cavitation often puts a limit on the maximum attainable ductility. It also can reduce the post-formed ambient temperature mechanical properties. The possible degradation of service properties may be particularly serious in the case of the 7475-Al type alloys, since they are often used for structural components.

Recently, however a method has been demonstrated that eliminates or minimizes this cavitation by the simultaneous imposition of a hydrostatic pressure during the superplastic deformation. Bampton, Mahoney, Hamilton, and Ghosh at Rockwell Science Center were the first to demonstrate that the extent of cavitation in this alloy is significantly reduced by the application of a hydrostatic pressure during superplastic deformation. However, their work did not establish unambiguously if the decrease in cavitation phenomenon was due to a decrease in nucleation of cavities or growth of cavities or both. The engineering significance of further studies in such area in the context of metal forming process at high temperature is obvious. In a more fundamental context such studies may shed more light on the process of cavity growth by

diffusion-controlled and plasticity-controlled mechanisms and also on the possibility of a change in the rate-controlling growth mechanism as a function of cavity size.

The outcome of this investigation should have a broad generality. Whereas some superplastic alloys, e.g. Ti-6Al-4V, are composed of a two-phase matrix, others are composed of essentially a single-phase matrix. Typical examples for the latter type are 7475 Al or Al-Li alloys with Zr addition, having hard particles that pin the grain boundaries and minimizes the process of grain growth during superplastic deformation. These second type of alloy for structural application almost always contains dispersions of both intermetallic particles and age-hardening precipitates. One expects that the hard particles located at grain boundaries to decohere during grain boundary sliding (in superplastic flow) and thereby help in nucleating the cavities.

This type of investigation for superplastic deformation under superimposed hydrostatic gas pressure has the potential of significantly reducing the incidence of cavitation. The approach may produce a decent integration of basic materials science principles and a viable forming procedure. A better understanding of the precise role played by hydrostatic pressure on such cavitation phenomenon will assist in utilizing the full potentials of the new generation of superplastic alloys.

This report presents the outcome of our recent preliminary investigation in this area. We have designed and built a high temperature, high pressure tensile test assembly where specimens can be pressurized by argon gas while being deformed in superplasticity using a specially modified Instron machine. The test run is controlled by a computer with a fairly fast digital data acquisition system. The dedicated constant-crosshead speed Instron machine was modified so as to run at constant strain rate.

The results on our investigation on 7475-T6 aluminum alloy is being presented in two parts. In Section 4 we present the results of our investigation on the "Superplastic Deformation Behavior of a Fine-Grained 7475 Aluminum Alloy." This formed the essence of the dissertation work of M. K. Rao. In the following Section 5, we present the superplastic deformation mechanism as well as the superimposed hydrostatic pressure of argon gas on cavitation phenomenonon in 7475-T6 aluminum alloy. The investigation involving gas pressurization is the outcome of dissertation work of Jerrold E. Franklin.

Significant Results For The 7475-T6 Alloy

1. The experimental results clearly reveal that the 7475 alloy undergoes strain hardening during superplastic deformation. Strain influences both the strain-rate sensitivity and the activation energy for superplastic flow.

2. Contrary to the prediction of the usual models on superplasticity, the grains do become elongated in this alloy with increasing strain. There is considerable dislocation activity in the matrix. Dislocations interact particularly with Cr-rich particles in the grain.

3. The activation energy for superplastic flow in this alloy is close to that for lattice diffusion. Most of the theoretical models on superplasticity predict an activation energy equal to that for grain boundary diffusion.

It is suggested that the rate controlling step in the deformation mechanism in this alloy is the climb of dislocations over the Cr-rich particles in the grain interior. These dislocations eventually reach the grain boundary where they climb into the boundary and are annhilated. However, in these sequential processes, the rate is controlled by the slower process of the climb motion of the dislocations over the Cr-rich particles.

Hence, the activation energy of the superplastic deformation will correspond to that for lattice diffusion.

4. A true steady-state microstructure is never achieved in this alloy. The dislocation density increases with strain, producing significant level of strain hardening. This strain-hardening in the present investigation is not due to grain growth.

5. The experimental results correlate reasonally well with the broad predictions from a theroetical model (Arieli-Mukherjee) that puts some emphasis on the grain boundary substructure in the details of the accomodation process of grain boundary sliding.

Significant Results of the Gas Pressurization Experiments (7475-T6 alloy)

1. Preliminary studies indicated that the constituent particles present in this alloy are intimately involved in the nucleation of cavities during superplastic deformation. TEM investigations revealed grain boundary cavities at an early strain associated with such particles.

2. Both optical microscopy and TEM study revealed a process of interlinkage of cavities at atmospheric pressure as a function of strain. The cavities link up and elongate along the direction of tensile axis. This suggests that the cavities probably grow by continuum hole growth process.

3. The superplastic ductility in this alloy is obviously increased very substantially by superimposing argon gas pressure. The most remarkable aspect of this extraordinary ductility is the fact that it has been achieved by virtually eliminating internal grain boundary cavitation.

4. The ongoing investigation will now try to ascertain if the effect of superimposed gas pressure is to reduce the rate of nucleation of cavities, the rate of growth of cavities or both.

SECTION 2

STRAIN RATE SENSITIVITY AND ITS DEPENDENCE ON MICROSTRUCTURAL EVOLUTION DURING SUPERPLASTIC DEFORMATION IN Ti-6Al-4V ALLOY

by

Michael Meier and Amiya K. Mukherjee

SUMMARY

A study of the superplasticity of Ti-6Al-4V has been done where the parameters for the Mukherjee, Bird, and Dorn equation are evaluated under conditions that include strain hardening, strain softening and steady state deformation behaviors. Microstructural aspects are investigated in order to account for nonsteady state deformation behaviors and the temperature dependence of the stress exponent. Mechanical testing consisted of three types of true strain rate tensile test, (a) constant true strain rate, (b) cycling the strain rate at 1048, 1098, 1148 and 1198°K, and (c) temperature change tests in the range of 1063 to 1208°K but at constant true strain rate. The results showed that the stress exponent, n, which is inverse of the strain rate sensitivity m, is independent of strain but varies with temperature in a manner that strongly suggests that the role of the volume fraction of phases is directly responsible for the strain rate sensitivity of this alloy. However, the exact manner in which n varies with temperature depends on the test used to measure it. These differences reflect on the true nature of n and has important implications on the significance attached to it. On the other hand, the activation energy appears to be independent of strain, strain rate and temperature. However, the values obtained are too high to be correlated with self diffusion.

The grain size sensitivity is equal to 1, which is lower than that normally reported for superplasticity and diffusion controlled creep. Microstructural evolution during superplastic deformation is dominated by recrystallization, but also includes some redistribution of the phases and a minor amount of grain growth. These observations, coupled with the correlation between volume fraction and the stress exponent requires that our theories regarding the mechanisms for superplastic deformation must incorporate the different roles of each phase present in the alloy. The behavior of this alloy fits rather well the description of the properties of heterogeneous aggregates. A suitable description of the behavior of Ti-6Al-4V is given in terms of the properties of the constituent phases, volume fraction of phases, grain sizes, and the effects of strain rate, stress and the processes of stress redistribution during deformation.

In addition to the analysis of the deformation process, recommendations are made regarding the optimum conditions for superplastic forming. Maximum ductility correlates with temperatures and strain rates that produce either steady state or strain hardening behaviors (strain exponent, h, is equal to or greater than zero). An accurate, empirical function for h in terms of strain rate and temperature is given.

This line of research is being continued using an iron modified version of Ti-6Al-4V. Its lower beta transus and lower forming temperatures makes it an ideal alloy for continuing work on developing methods for predicting the high temperature deformation behavior of multiphase alloys.

1. INTRODUCTION

Titanium alloys in general are relatively expensive and difficult to fabricate. Fortunately, they are superplastic. The most widely used titanium

alloy is Ti-6Al-4V. It has good corrosion resistance and twice the strength of unalloyed titanium. It has been on the market for over thirty years. Its superplastic characteristics were first investigated 10 years after it became generally available [1,2]. Superplastic forming titanium alloys is not hindered by the high strength, limited ductility and excessive springback encountered using conventional forming methods. Superplastic forming has also been combined with diffusion bonding to produce complex components at up to 40 percent savings in both materials and labor costs. In spite of the successes, Ti-6Al-4V still has a reputation for being "not well behaved." While the main characteristics of superplasticity are fairly well established, most reports on the superplasticity of Ti-6Al-4V do not fit the norm. Equation 1 is a constitutive equation that describes the relationships between the major metallurgical parameters, (d) grain size, (D) diffusivity, (A) structure and deformation parameters, (σ) stress, ($\dot{\varepsilon}$) strain rate and (T) temperature for a specified rate controlling high temperature deformation process.

$$\frac{\dot{\varepsilon}kT}{DGb} = A\left(\frac{\sigma}{G}\right)^{n}\left(\frac{b}{d}\right)^{p} \qquad (1)$$

The parameters that are used to characterize the high temperature deformation behavior of a material are the stress exponent, (m=1/n), grain size sensitivity, p, the activation energy, Q (which is usually related to the activation energy for self diffusion) and the structure sensitive parameter, A. These parameters are considered to be constants for steady state deformation governed by a single rate controlling mechanism. Typical values of these parameters are summarized in table 1. However, in studies on the

superplasticity of Ti-6Al-4V it has reported that the stress exponent varies with both strain [3,4,5] and temperature [2,4,6]. In addition, the usual correlation between a maximum value of the stress exponent and the maximum ductility is applicable only at a specified temperature [4]. The values reported for the activation energy vary from around 125 kJ/mole to as high as 975 kJ/mole. These are summarized in table 2. Most of the activation energies reported are either near or well above the upper limits of the controversial range of activaton energies for self diffusion (approximately 250 kJ/mole for lattice diffusion). The grain size sensitivity, though not often evaluated, is reported to be approximately 2, which is normal, but the value reported for A tends to be too high and can vary with strain. Concurrent grain growth, dynamic recrystallization, the presence of impurities and the presence of a second phase have all been suggested as reasons for the strain dependence of the otherwise constant characterizing parameters, as well as the anomalous behavior of n and the high values of Q [7,8,9].

The purpose of this study is to investigate the microstructural aspects that are significant with respect to the superplastic deformation of Ti-6Al-4V. To do this it is necessary to first characterize the superplastic behavior in terms of parameters that are not functions of strain, then measure the strain dependence of the flow stress and finally look into the microstructural aspects that are responsible for both the strain and temperature dependence of the superplastic deformation of Ti-6Al-4V.

2. PROCEDURE

The alloy used in this research was a fine grained Ti-6Al-4V provided by Adi Arieli at Northrop Aerospace Corporation, Los Angeles. The as received material was annealed at 1198°K for from 1 to 10 hours in an argon atmosphere

to produce a microstructure containing approximately 50 percent beta and alpha grain sizes from 3.2 to 6.4 microns. These specimens were used for mechanical testing. Other specimens were annealed for from 1 to 100 hours at temperatures from 1048 to 1198°K to provide data on the grain growth kinetics and equilibrium volume fraction.

All mechanical testing was done using a MTS closed loop servo-hydraulic test system. A PDP 11/04 minicomputer provided system control, data acquisition, and some data analysis functions. A quad elliptical radiant heating furnace was used to provide the test temperature. This furnace was capable of bringing the specimen and associated hardware up to the test temperature within seven minutes, maintaining that temperature to within one degree centigrade and allowing the specimen be cooled quickly enough to avoid significantly altering the microstructure of the specimen as it cooled through the alpha/beta region. Accuracy of temperature control was at least as good as the accuracy of the K-type thermocouples used.

The computer was programmed to conduct constant true strain rate tensile tests. All testing was conducted at temperatures between 1048 and 1208°K and strain rates between $2x10^{-5}$ and $2x10^{-2}$ per second. Three different types of tensile tests were used. The primary type was one which was conducted at constant temperature and strain rate for true strains up to 1.0 or fracture, which ever occurred first. These tests provided the basis for most of the analysis of the characterizing parameters, n, p, Q, A and in particular, h. The second type of tensile test was employed primarily to verify previous observations of the temperature and strain dependences of the stress exponent. This involved testing at a given constant temperature while cycling the strain rate between two strain rates. These tests were conducted

over a range of temperatures and for two sets of strain rates. The third type of tensile test was used to verify the results of previous activation energy calculations. These tests were conducted at constant strain rates, but the temperature was changed periodically by 10 to 15°K. These temperature changes were accomplished within approximately 30 seconds.

All metallography was done using an optical microscope. Quantitative metallography involved measuring the volume fraction of phases by point count and grain size measurements by both lineal intercept and grain area measurements combined with the Johnson-Saltykov method of correcting for the third dimension.

4. RESULTS

Stress-Strain Behavior

Figure 1 summarizes the results of all of the constant strain rate tensile tests. It shows the effects of strain rate, temperature and strain on the stress. For each temperature there is a region where the slopes of the lines are maximum. This region is generally in the vicinity of strain rate equal to 2×10^{-4} per second. At the higher two temperatures, this region is also the region where steady state type of flow behavior is seen. At 1198°K this behavior occurs within a very narrow range of strain rates. At 1148°K this region becomes broader, while at even lower temperatures this behavior diminishes and the steady state behavior becomes a brief transition between hardening and softening behaviors. It is interesting to note that down to 1148°K the steady state behavior involves essentially the same stress.

At strain rates lower than those which produce a steady state behavior, strain hardening behavior is observed. Above this strain rate strain softening occurs. In order to evaluate the charcterizing parameters, n, p, Q,

etc., it is necessary to temporarily ignore the effects of strain and focus on the behavior at low strains. Since it is not possible to get steady state behavior over a wide range of temperatures and strain rates the characterizing parameters are evaluated based on data obtained at low strains. Once these have been established, the strain effects can be measured and incorporated with the previous results. Figure 2 shows a plot similar to figure 1 except that it is based on a stress close to the yield stress. Figure 2 clearly shows that at intermediate and low strain rates there is a split in the behavior of this alloy that occurs between 1098 and 1148°K, as evidenced by the difference in the shape of the $\log\dot{\varepsilon}$ versus $\log\sigma$ curves in that region.

Stress Exponent

In principle, the slope on the $\log\sigma$–$\log\dot{\varepsilon}$ plot is equal to the stress exponent, n, which is the inverse of the strain rate sensitivity, m. Figures 3a and 3b show plots of the maximum slopes in the $\log\sigma$–$\log\dot{\varepsilon}$ data plotted in figure 1 and n_o measured from figure 2. Figure 3a indicates that it varies with temperature, a characteristic that is not often reported. It implies that either n itself is a function of temperature, or that more than one deformation mechanism is responsible for the observed behavior and that the relative contributions of each mechanism is changing with temperature. Since little is known about the real significance of n and the change in n with temperature follows the change in volume fraction of the beta phase with temperature, the latter explanation is preferred. Figure 3b shows that n_o changes abruptly at about 24 volume percent beta.

The strain rate cycling tests indicate that the stress exponent, n_c is not a function of strain. Figure 4 shows a typical stress-strain curve produced from a strain rate cycling test. The stress exponent can be measured eight times during the test. In all tests it was shown that regardless of the

net strain behavior, hardening, softening or steady state, n_c is constant with respect to strain.

The results of the strain rate cycling tests do not quite agree with the results just discussed showing a temperature dependence of n_o plotted in fig. 3a. Figures 5a and 5b show plots of n_c against temperature and volume fraction beta, respectively. These show that for a given temperature, or volume fraction and narrow range of strain rate that there is a minimum value for the stress exponent. The conditions that produce this minimum happen to coincide with the conditions that produce steady state deformation. This indicates that there is a unique relationship between the strain rate, temperature, volume fraction beta and minimum n_c that produce steady state deformation.

The values and temperature dependencies of the stress exponent appear to depend on the method that was used to evaluate it. This has important implications regarding the physical significance of the stress exponent. The disagreement between the temperature dependencies of n_o and n_c can be explained by the differences in the types of tests used to measure it. The stress exponent n_o is based on the stress early in a test conducted at one strain rate. Each stress and strain rate used to calculate n_o came from an independently conducated experiment and therefore represents the deformation processes and microstructural evolution associated with each particular test. On the other hand, n_c is a measure of the material's response to an abrupt change in the strain rate, and consequently the microstructural aspects that accommodates and/or resists sudden change in strain rate. Possibilities are readjustments in dislocation density, overcoming the weaker barriers to grain boundary sliding and redistributing the alpha and beta grains. These are not

investigated here. However, it is clear that the stress exponent that represents the stress at which the characteristic flow behavior begins decreases with temperature in a manner, that closely follows the volume fraction present at that temperature, while the stress exponent, n_c, that describes the sensitivity to changes in stress or strain rate is independent of strain, has a minimum value when steady state deformation takes place, and is associated with a specific volume fraction of phases for the given conditions of deformation.

Temperature Dependence

Figure 6 shows the plots used to determine the activation energy for the high temperature deformation of Ti-6Al-4V. These results are from several types of tests, including the temperature change tests. They all show a good fit to a Arrhenius type of function with an activation energy consistently within the range of 293 to 355 kJ/mole. This is too high to be correlated with self-diffusion in this alloy, and hence, with models for creep and superplasticity. Although several possible reasons for having an unusually high activation energy have been cited [7, 8], table 2 illustrates the fact that the issue of the activation energy for Ti-6Al-4V is far from being settled. Without having a unique thermally activated process to correlate these findings with, one is reluctant to even call these numbers activation energies in our alloy, where there is a significant amount of microstructural evolution during deformation and, for the time being, must interpret these numbers as parameters that describe the net temperature dependence of deformation of this alloy. These results do, however, match the results of a correlation done by Bryant [9] who showed that for a wide variety of deformation conditions, the activation energy is either 350 or 732 kJ/mole.

It is curious that while volume fraction and stress exponent both change with temperature, the activation energy does not. It was expected that the activation energy would also change with the volume fraction to reflect the relative contributions of each phase. The fact that it didn't, suggests three possibilities. First, the activation energy for whatever deformation process is rate controlling in the alpha and beta phases is equal. Second, that only one phase is being deformed, and it is the temperature dependence of the deformation of that phase that has been measured. Finally, the rate controlling process takes place in a region that is common to both phases and thus may have its own characteristic temperature dependence. Such places are grain boundaries, and in particular, those grain boundaries that are also interphase boundaries. These microstructural features vary less with temperature than volume fraction, particularly at low temperatures where the small amount of beta exists as a grain boundary phase, may have their own composition and structure [10,11], and are the most important microstructural feature in terms of the grain boundary sliding that is characteristic of superplasticity.

Microstructural Parameters

The microstructural parameters in equation 1 are p, A and (to some extent) D_o. The grain size sensitivity, p, was found to be between .85 and 1.2. This lower grain size dependence is consistent with the finding that volume fraction is also a factor affecting the properties of Ti-6Al-4V. Therefore, characterizing the microstructure in terms of the grain size alone is not sufficient for correlating the effect of microstructural variables on the superplasticity of this alloy. There are two grain sizes to consider, one for each phase, and the properties of each phase are different. A word of

caution will be appropriate regarding the value of p given here; it was measured based on the size of the alpha grains only. The beta grain size was not measured due to the difficulty of distinguishing between grains of the alpha prime, a martensitic structure that the high temperature beta phase transformed to during cooling after the tensile test. Also, equation 1 has no provision for more than one phase or grain size, so one should be careful not to apply the traditional interpretation to this measurement of the grain size sensitivity.

The structure sensitive parameter A was evaluated without considering the grain size. Also, since the value of D_o is not known, this parameter, which will now be called A', incorporates all structural terms;

$$A' = A\, D_o\, (b/d)^p \qquad (2)$$

The results show that A' is equal to 1 and independent of temperature. Based on this, A is estimated to be on the order of 10^4, which is higher than that given in any of the models for superplasticity, but it is not uncommon to get such high values for A. It does show, however, that when the temperature dependence of n is considered, the structure dependence of superplasticity (as depicted by A') is constant. This suggests that the parameter n has already incorporated the volume fraction dependence of the properties (since it is known that the structure is temperature dependent through its volume fraction of phases) while the structure parameter, A', was not. These parameters appear to be more interrelated than equation 1 would indicate.

Strain Dependence

A quantitative measure of the strain dependence of deformaton is given by the strain exponent h. It is defined in an expression of the form;

$$\sigma = K \dot{\varepsilon}^{m} \varepsilon^{h} \qquad (3)$$

A plot of h that represents the strain hardening, softening and steady state behaviors seen in figure 1 is shown in figure 7. Positive values of h indicate strain hardening, h equal to zero indicates steady state behavior and negative values of h, strain softening. An analysis of this data shows that the slopes in the linear portions of figure 7 is proportional to the temperature while the intercept of those lines with the h=0 axis is also a simple linear function between the temperature and the log of the strain rate. These are combined in equation 4 to give a general expression for the strain dependence of deformation in terms of temperature and strain rate.

$$h = (10.25-0.0118\ T)\log(\dot{\varepsilon}) - (T-1399)/63.6 \qquad (4)$$

This equation is valid for only the linear portion of the lines, which excludes any values of h less than about - 1.5 but covers all the range that is relevant to superplastic deformation. Although equation is empirical, it is a first attempt to characterize nonsteady state superplastic type deformation; fits the data well; covers a wide range of temperature, strain rates and deformation processes; is associated with the stress exponent (n_c); and is useful in predicting the extent of strain hardening or softening behaviors and in determining the optimum conditions for superplastic forming. An explanation for the behavior of h is not trivial due to the fact that microstructural evolution involves several microstructural characteristics. Grain growth or refinement, recrystallization, and the different roles each phase plays in the deformation process.

Microstructural Evolution

Figures 8 and 9 shows how the equilibrium volume fraction of phases varies with temperature. The microstructural evolution during superplastic flow shows that recrystallization takes place to adjust the volume fraction of phases to its new equilibrium at the test temperature. Figure 10 shows the microstructures produced after deformations of 1.0 true strain, strain rate equal to 2×10^{-4} per second and four different temperatures. The differences in volume fraction can be clearly seen. Changes in the grain size are also apparent, but part of this grain size modification can be attributed to recrystallization, since studies of the grain growth kinetics at these temperatures do not show such dramatic changes in grain size during the brief hour or so that the specimens were at the test temperature. Figure 11 shows that, in fact, a significant degree of microstructural evolution has taken place during the short time before the tensile test when the specimens, associated grips and load train were being heated to the test temperature.

5. DISCUSSION

A comparison of tables 1 and 3 show the differences in the behavior of a typical superplastic alloy and that for Ti-6Al-4V. Ti-6Al-4V, while being very superplastic, is not a typical superplastic alloy. Its stress exponent, n, is only nominally equal to 2. It is not a constant either, as it varies with temperature, or volume fraction, strain rate and the method of testing used to evaluate it. The activation energy is high by a factor of two and the grain size sensitivity is low. In addition, there is a strain exponent that usually is not considered in either studies like this or the models for superplasticity and creep. It has been shown to vary with temperature and strain rate and has also been shown to have some points in common with the

stress exponent, n_c. The strain exponent is a parameter that describes the effect of microstructural evolution on the deformation behavior. A correlation between the strain exponent and microstructural evolution has not been possible, due to the fact that there are two microstructural processes to account for grain growth and changes in the volume fraction of phases, processes which are not independent of each other and that the deformation behavior is dependent on the volume fraction of the phases present. The situation is more complicated than the one that was expected (microstructural evolution involving only grain growth, no dependence of properties on volume fraction). In order to adequately describe the behavior of this alloy, it is necessary to broaden the scope of the existing models and constitutive equations so that they address the material as the two phase alloy that it is, each phase playing a different role in the deformation behavior. Tensile tests like those conducted in the study measure bulk properties, stress, strain, overall temperature dependence, etc., from which an attempt is made to deduce the fundamental micromechanisms that are responsible for the observed behavior. For single phase and multiphase alloys, where either the properties of the phases are similar or the amount of one phase is small enough to be negligible, this is a relatively straight-forward process. However, in cases like the one at hand (where the material is an aggregate of two phases, each with distinctly different properties, structure and composition) the significances of the microstructural parameters grain size(s), volume fraction and the distribution of the phases are different from the previous case; and it is necessary to incorporate these factors into the analysis of material behavior. This would require application of the methods developed in the mechanics of solids field. A brief review of this literature indicates that

little of this work ever discusses material behavior in terms of physical processes. Ladanyi [13], in a review of the behavior of frozen soils, has discussed these factors in terms that seem especially appropriate for characterizing the creep and superplastic behaviors of Ti-6Al-4V. The analogy between the high temperature behavior of a high performance aerospace alloy and frozen soils is not as peculiar as it might seem. Frozen soils are, afterall, aggregates of two distinctly different phases where the ice phase is known to creep by a dislocation process, n being equal to three, and is at a high homologous temperature. Ladanyi comments on the similarities between the behavior of frozen soils and the creep of metals and the behavior of artificial particulate composites, but notes that the primary differences are: 1) that soils do not obey an absolute reaction rate as metals do and 2) that the effect of pressure melting, which in frozen soils is considerable, but in metals is negligable. Gegel et al., [29] finds that pressure induced phase transformations in Ti-6Al-4V do occur at triple points and is significant enough to consider as part of the overall deformation behavior. However, there are some important similarities between the behavior of soils and the behavior Ti-6Al-4V in terms of the following seven items.

1. Properties of the individual phases: the behavior is dominated by the properties of the softer phase, which accomodates most, if not all of the strain.

2. Phase proportion: strength varies with volume fraction of the phases present. A few percent addition of the harder phase causes the strength to decrease, due to grain refinement and grain boundary sliding. Further increases in the amount of the harder phase causes strength to

increase by a dispersion hardening type of mechanism. At about forty volume percent of the harder phase, the strength increase is due to interparticle friction. As the amount of the harder phase increases further, the properties of the material approach that of the harder phase. It forms a continuous skeleton that is capable of carrying the load without any contribution from the softer phase.

3. Size and shape of the grains of the harder phase: which dictates their ability to rotate and slide past each other, or to lock up and resist further deformation.

4. Physio-chemical nature of the grain boundaries: particularly at the interphase boundaries, determines what is effectively a "coefficient of friction" for grains that are in sliding contact with each other.

5. Strain rate: must be low enough to allow the softer phase to accomodate the strain. If the strain rate is too high then fracture will occur through the softer phase.

6. Strain: accomodated primarily by the softer phase. The harder grains are suspended in the matrix of the softer phase. Periodically the harder grains come into contact with each other and, depending on the angle at which they contact, the "coefficient of friction," and the degree to which neighboring grains of the harder phase restrict its movement, these grains will either slide past each other without raising the total stress appreciably, or they will lock up, prevent further straining and increase the stress. If the stresses become high enough, the harder grains might fracture and the smaller pieces will slide past each other relieving the stresses. The degree of interaction between the grains of the harder phase increases as the amount of softer phase decreases. The softer phase acts to separate the

harder grains and to accomodate their relative movements. Lack of a sufficient amount of the softer phase, not only results in an increase in the stress but also the amount of cavitation that would occur between the alpha grains.

7. Stress distribution: mechanical testing only measures the total stress on the material. Within the specimen stress concentrations occur at triple points and interphase boundaries and can raise the local stresses significantly. In frozen soils the increase can be anywhere from a factor of 10 to 500, depending on whether the behavior is elastic or viscoelastic.

This short list contains the major components for explaining the whole range of behaviors observed for Ti-6Al-4V. Each item alone is a good point to investigate in order to determine what are the actual micro-mechanisms for superplasticity of this alloy.

The parameters measured in the course of this research do not quite fit any of the usual patterns, and as a result it is not possible to conclusively correlate its behavior to any of the established models for superplasticity. Two approaches that are being used with some success are the iso-stress and iso-strain approaches. The key assumption in both cases is that, in essence, only one phase determines the overall behavior and that the amount of interaction between the two phases is unimportant. These two cases were mentioned in items 1 and 2 above. However, they are limited to only those situations where the volume fraction of only one of the phases is important and does not deal with cases where both phases either interact or make similar contributions to the deformation behavior. This region is both interesting and important in terms of lowering the superplastic forming temperatures and alloy design, in general. For a better understanding of the whole picture it

would be necessary to work out the mechanics of the actual two phase structure, in general terms, after which it might be possible to isolate the roles and contributions of the deformation responsible for the "total" or externally visible behavior. Often it has been found that structurally complex materials (eutectics, particle bearing, multiphase materials) have, upon examination, revealed themselves in ways that make it easy to make meaningful correlations with the behaviors observed in other materials. Unfortunately, that is not the case here. This alloy is not homogenous, nor is it a simple heterogeneous alloy containing a minor fraction of relatively small and inert particles; and measurements of the macroscopic behavior in terms of the total stress, strain, etc., have not revealed which microscopic, atomistic processes are rate controlling. However, the parameters measured in this research are valid and useful descriptions of the deformation behavior of Ti-6Al-4V, and several approaches that might be more useful for studying the fundamental deformation behavior of Ti-6Al-4V and other similar alloys.

Optimum Conditions for Superplastic Forming

From all of the results obtained it is possible to make some general recommendations for the superplastic forming Ti-6Al-4V. These recommendations are based primarily on the stress-strain curves, measures of ductility and the $\log\sigma$-$\log\dot{\varepsilon}$ curves. The characterizing parameters (A, n, p, h, Q, etc.) can be used to give a more specific prediction of the deformation characteristics.

The forming temperature should be at least 1148°K. Forming at

temperatures below 1148°K would likely produce unacceptable results due in part to the decreased ductility and in part due to cavitation. At temperatures above 1148°K (and at the appropriate strain rate) strains greater than 1.0 (172 percent engineering strain) are achieved. At higher temperatures not only such high values of strain are attainable, but most notable was that up to a strain of 1.0 it was possible to completely avoid localized deformation. The other advantage of forming at higher temperatures is that the optimum strain rate is higher. Assuming an activation energy of 365 kJ/mole, a change in forming temperature from 1148°K to 1198°K results in an increase in strain rate by a factor of about 4.5. However, at the higher forming temperature it becomes more important that the strain rate not exceed a critical value that yields a negative value of strain hardening exponent, as ductility decreases rapidly as the $\dot{\varepsilon}$ is increased.

The optimum strain rates are equal to or less than the strain rate that results in a steady state type of behavior, i.e. the strain hardening exponent h, is zero. This strain rate varies with temperature and can be determined using the general equation for h, equation (16). An alternative to selecting a specific strain rate is to deform the material under stresses of 10 to 20 MPa. For temperatures from 1148°K to 1198°K, the optimum strain rates and maximum ductilities correspond to this range of stress.

It is still important to have a fine grained microstructure since the strain rate is roughly proportional to the inverse of the grain size. In addition to the grain size requirement it is important to have, at the very least, 25 volume percent beta; and the volume fraction should be close to that of the equilibrium volume fraction at a given forming temperature. Prior

heat-treatment to get the required volume fraction is not necessary and considering the accompanying increase in grain size that would occur, is discouraged. Normally, it should be sufficient to simply hold the material in preheated dies for a short time before starting the actual forming process. Superplasticity is a process that takes place primarily at the grain boundaries. The most dynamic aspects of microstructural processes (i.e., grain growth and recrystallization) also take place at the grain boundaries; so it follows that it is not necessary to have a particularly stable microstructure in order to get good superplastic behavior, as long as the microstructure does not evolve into one that is actually resistant to superplastic deformation (i.e., large grains, low volume fractions of the beta phase). A cold worked, fine grained microstructure should be an excellent starting material. It isn't necessary to perform a recrystallization anneal prior to the forming operation in order to obtain equiaxed grains since the two processes will occur concurrently and symbiotically during the forming operation.

6. CONCLUSION

An attempt has been made to characterize the superplasticity of Ti-6Al-4V using conventional assumptions that the process of analyzing the macroscopic behavior, so as to reveal the fundamental processes that control the deformation behavior, is a rather straight-forward one and that there was no need to differentiate between the roles that the constituent phases assume. However, the results (primarily the temperature dependence of the stress exponent(s) and the low sensitivity to grain size) suggest that the

behavior of this alloy does indeed depend on the proportions and properties of the phases present during deformation. In order to characterize the behavior of this alloy over a wide range of temperatures and microstructures, it is necessary to deal with this material and others like it in the context of heterogeneous materials. Although the results presented here might not constitute conclusive proof of the aggregate nature of the properties of Ti-6Al-4V, the failure of the original approach, coupled with the similarities with the general behavior of heterogeneous, aggregates together form a very reasonable basis for this interpretation of the behavior of Ti-6Al-4V. It also helps to define the approach to be used related work on an iron modified version of the Ti-6Al-4V base alloy. This alloy has a lower beta transus, which is associated with its lower superplastic forming temperature. Testing this alloy at lower temperatures but identical volume fractions of beta, will make it possible to differentiate between temperature and volume fraction effects, verify the results regarding Q and h and to begin to develop a general model for the high temperature deformation of multi-phase alloys.

In addition to a characterization of the behavior of this alloy (in terms of parameters of a constitutive equation), the results also make it possible to give some fairly explicit recommendation regarding the optimum conditions for superplastic deformation. These include an expression that predicts the amount of strain hardening or strain softening that will occur, descriptions of the significance of an unstable microstructure and prior thermo-mechanical processing.

REFERENCES

1. J. E. Lyttle, G. Fisher and A. R. Marder, Journal of Metals, 52 (1965) 1055.

2. D. Lee and W. A. Backofen, Transactions of the Materials Society, AIME, 239 (1967) 1034-1040.

3. N. Furushiro, H. Ishabashi, S. Shimoyama and S. Hori, Titanium '80 Science and Technology, ed. H. Kimura and O. Izumi, The Metallurgical Society of AIME, Warrendale, PA, (1980) 993-1000.

4. R. R. Boyer and J. E. Magnuson, Metallurgical Transactions A, 10A (1979) 1191-1193.

5. B. Gurewitz, Ph.D. Dissertation, Department of Mechanical Engineering, University of California, Davis, CA, (1984).

6. T. L. Mackay, S. M. L. Sastry and C. F. Yolton, Technical Report AFWAL-TR-80-4038, Wright-Patterson Air Force Base, Ohio, (1980).

7. W. D. Ludemann, L. A. Shepard and J. E. Dorn, Transactions of the Metallurgical Society of AIME, 218 (1960) 923-926.

8. R. G. Menzies, J. W. Edington and G. J. Davies, Metal Science, 15 (1981) 210-216.

9. W. A. Bryant, Journal Materials Science, 10 (1975) 1793-1797.

10. C. G. Rhodes and N. E. Paton, Metallurgical Transactions A, 10A (1979) 209-219.

11. C. G. Rhodes and N. E. Paton, Metallurgical Transactions A, 10A (1979) 1753-1758.

12. R. T. DeHoff, F. N. Rhines, Quantative Microscopy, McGraw-Hill, New York, (1968) 168-181.

13. B. Ladanyi, Mechanics of Structured Media, Part B, ed. A.P.S. Selvadurai, Elsevier Scientific Publishing Company, Amsterdam, (1981) 205-245.

14. C. M. Libanati and F. Dyment, Acta Metallurgica, 11 (1963) 1263-1268.

15. S. P. Murarka and R. P. Agarwala, Acta Metallurgica, 12 (1964) 1096.

16. F. Dyment and C. M. Libanati, Journal of Materials Science, 3 (1968) 349-359.

17. J. F. Murduck, T. S. Lundy and E. E. Stansbury, Acta Metallurgica, 12 (1964) 1033-1039.

18. S. Z. Bokshtein, Diffusion Processes, Structure and Properties of Metals, ed. S. Z. Bokshtein, Consultants Bureau, New York, (1965) 2-8.

19. T. A. Roth and P. Suppayak, Materials Science and Engineering, 35 (1978) 187-196.

20. R. L. Orr, O. D. Sherby and J. E. Dorn, Transactions of ASM, 46 (1954) 113.

21. G. Malakondaiah and P. Rama Rao, Acta Metallurgica, 29 (1981) 1263-1275.

22. K. C. Wu and R. E. Lourie, Metals Engineering Quarterly, 12 no. 3 (1972) 25-29.

23. H. Conrad, Acta Metallurgica, 6 (1958) 339-350.

24. A. Arieli and A. Rosen, Metallurgical Transactions A, 8A (1977) 1591-1595.

25. C. C. Chen and J. E. Coyne, Metallurgical Transactions A, 7A (1976) 1931-1941.

26. S.M.L. Sastry, P. S. Rao and K. K. Sankaran, Titanium '80 Science and Technology, ed. H. Kimura and O. Izumi, The Metallurgical Society of AIME, Warrendale, PA, 2 (1980) 873-886.

27. A. Arieli, B. J. McLean and A. K. Mukherjee, Res Mechanica, 6 (1983) 131-159.

28. M. T. Cope, M.S. Thesis, Department of Metallurgy, University of Manchester, (1982).

29. H. Gegel and S. Nadiv, Scripta Met, 14 (1980) 241-247.

TABLE 1
Nominal values of the parameters used in the Mukherjee, Bird, Dorn constitutive equation for high temperature deformation and the mechanisms that they identify.

Mechanism	A	n	p	Q
Nabarro-Herring Creep	7	1	2	Q_l
Coble Creep	50	1	3	Q_{gb}
Harper-Dorn Creep	10	1	0	Q_l
Superplasticity	200	2	2	Q_{gb}
Dislocation Viscous Glide Controlled	3	3	0	Q_l
Dislocation Climb Controlled	2×10^6	5	0	Q_l

($Q_{gb} \approx 0.6\ Q_l$)

TABLE 2
Activation energies for diffusion, creep and superplasticity of Ti-6Al-4V and some titanium alloys.

Q (kJ/mole)	Comments and Reference
Diffusion	
23	Ti^{44} tracer in alpha Ti. Libanati, Dyment (14)
variable	Based on Libanati and Dyment. Murarka, Agarwala (15)
150	Ti^{44} tracer in alpha Ti. Dyment, Libanati (16)
131, 251	Ti^{44} tracer in beta Ti. Murdock, Lundy, Stansbury (17)
159, 360	Autoradiographic technique on alpha prime and beta Ti. Bokshtein, Emel'yanova, Kishkin, Mirskii (18)
Creep	
D = -10.98E-7 + 7.85E-10 * T, D = -9.87E-7 + 7.64E-10 * T	Zero creep of pure Ti and Ti-6Al-4V, respectively, Q not given but temperature dependences are similar. Roth, Suppayak (19)
251, 335	Creep rupture of 99% Ti and Ti-D9 (95.7%). Orr, Sherby, Dorn (20)
121, 241	Low stress creep of alpha Ti, Q_{GB} below 970°K, Q_L above 970°K. Malakondaiah, Rao (21)
Superplasticity of Ti-6Al-4V	
$Q \sim Q_{SD}$	Superplasticity of Ti-6Al-4V. Lyttle, Fisher, Marder (1)
*	Strength inversion made calculation of Q "meaningless". Lee and Backofen (2)
219, 732	Higher Q at lower T and strain rates. Wu and Lowrie (22)
293	1033°K < T < 1213°K. Conrad (23)

188 + 19	Independent of stress and temperature. Arieli, Rosen (24)
356, 720	Correlation of results of 24 experiments using the Zener-Hollomon relation. Higher Q at higher T and strain rate. Bryant (9)
565, 963	Increases with decreasing stress. Chen, Coyne (25)
109, 419	Varied with stress and temperature, high Q related to microstructural modification. MacKay, Sastry and Yolton (6)
469, 573	Apparent temperature dependence of the strain rate.
278	Steady state, high stress and T.
188	Low T ($T<873^{o}K$) and low stress. Sastry, Pao, Sankaran (26)
335	Somewhat successful with correcting for concurrent grain growth. Arieli, Mac Lean, Mukherjee (27)
167, 243	Independent of stress from 6 MPa to 50 MPa, region 1, 2. Cope (28)
134-155, 180	Stress of 5 Mpa and 40 MPa respectively. Gurewitz (5)

TABLE 3
Values of the characterizing parameters for superplastic deformation of Ti-6Al-4V.

Parameter	Value	Comments
n	Nominally 2	Depends on how it was measured.
n_c	*	Varies with temperature, minima corresponds with steady state deformation, h=0.
n_o	2.45 to 1.24	Decreases with temperature (1048 to 1198°K) most of which takes place between 1123 and 1173°K which corresponds to 25% beta.
Q	293 to 356 (kJ/mole)	Fairly constant for temperatures between 1048 and 1198°K.
p	-1	Nominal. Based on alpha grain size only.
A	-10,000	Nominal. Estimated from A'=1.
h	(10.248-0.0118 T)log(c) - (T - 1399.04)/67.6	Empirical, applicable for temperatures between 1048 and 1198°K, and h greater than -1.5.

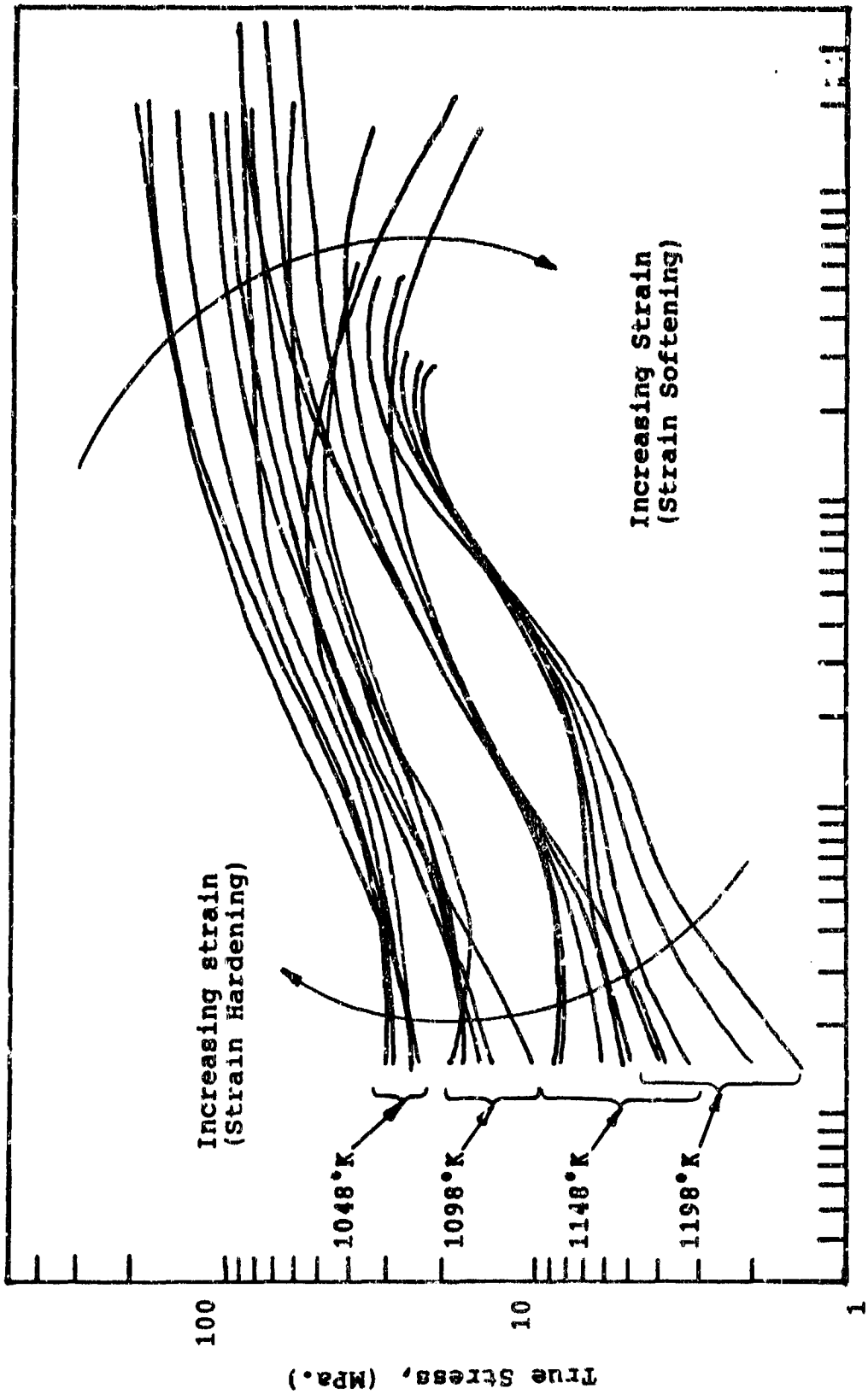

Figure 1. Compilation of results from the tensile tests showing the effects of strain rate, temperature, and strain on the stress.

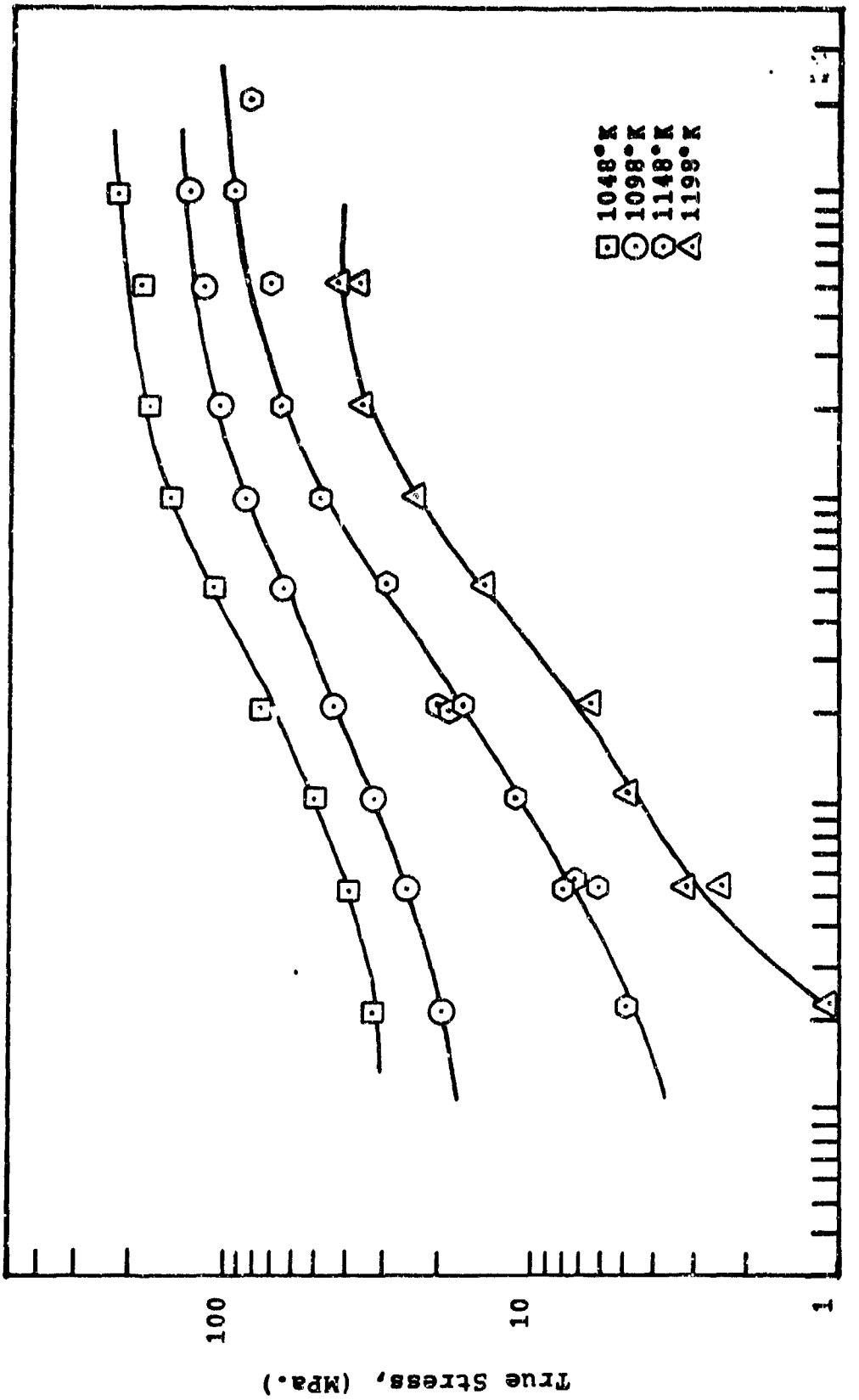

Figure 2. Log(σ)-log(ε̇) plot for stresses at low strains.

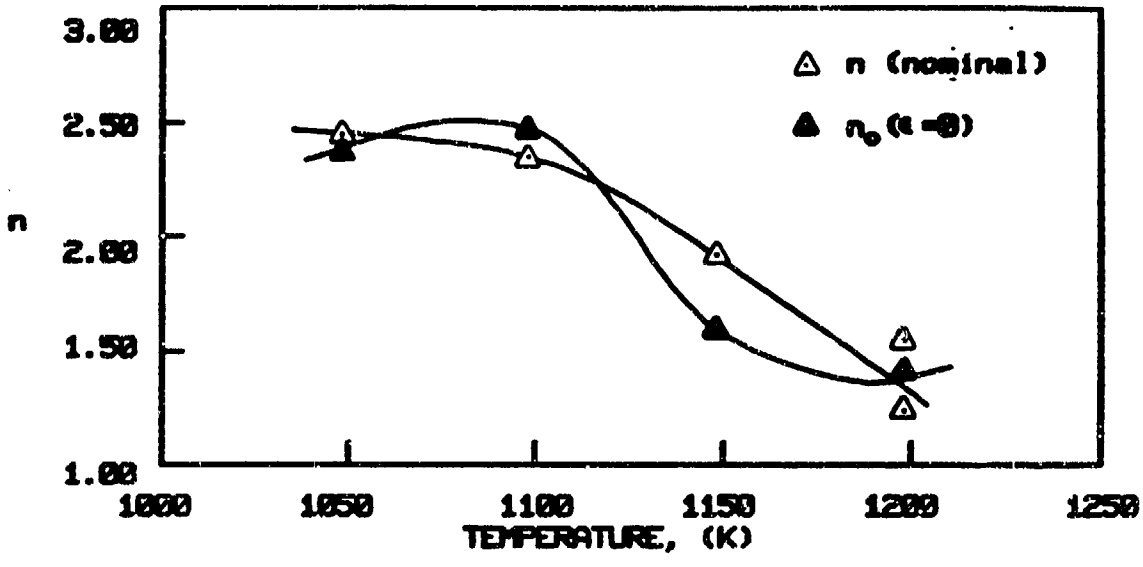

Figure 3a. Temperature dependence of the stress exponents n (nominal) and n_o.

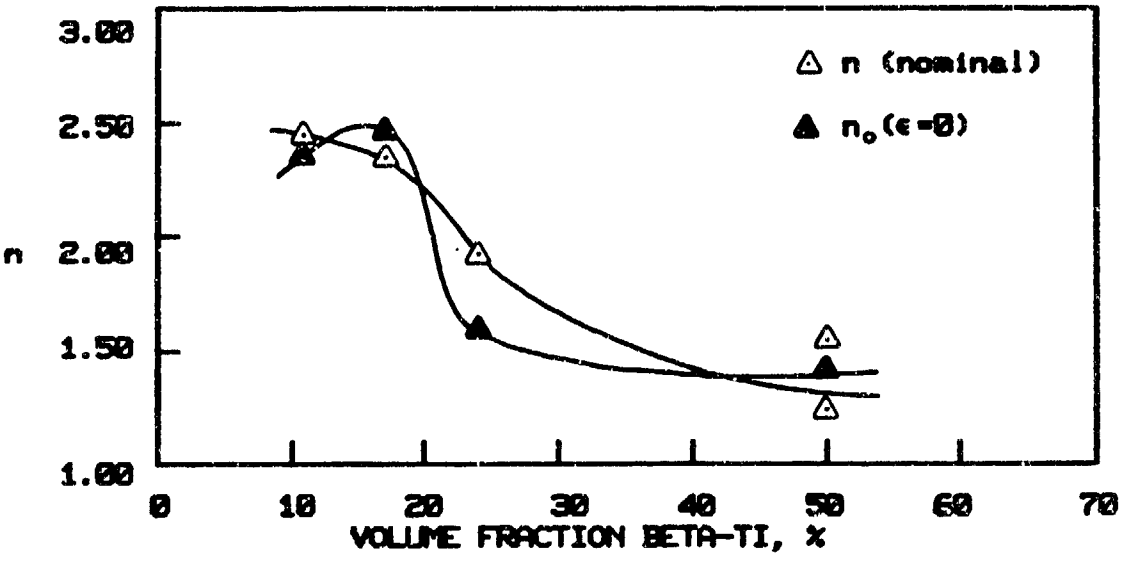

Figure 3b. Variation of the stress exponents, n (nominal) and n_o, with volume fraction of beta-titanium.

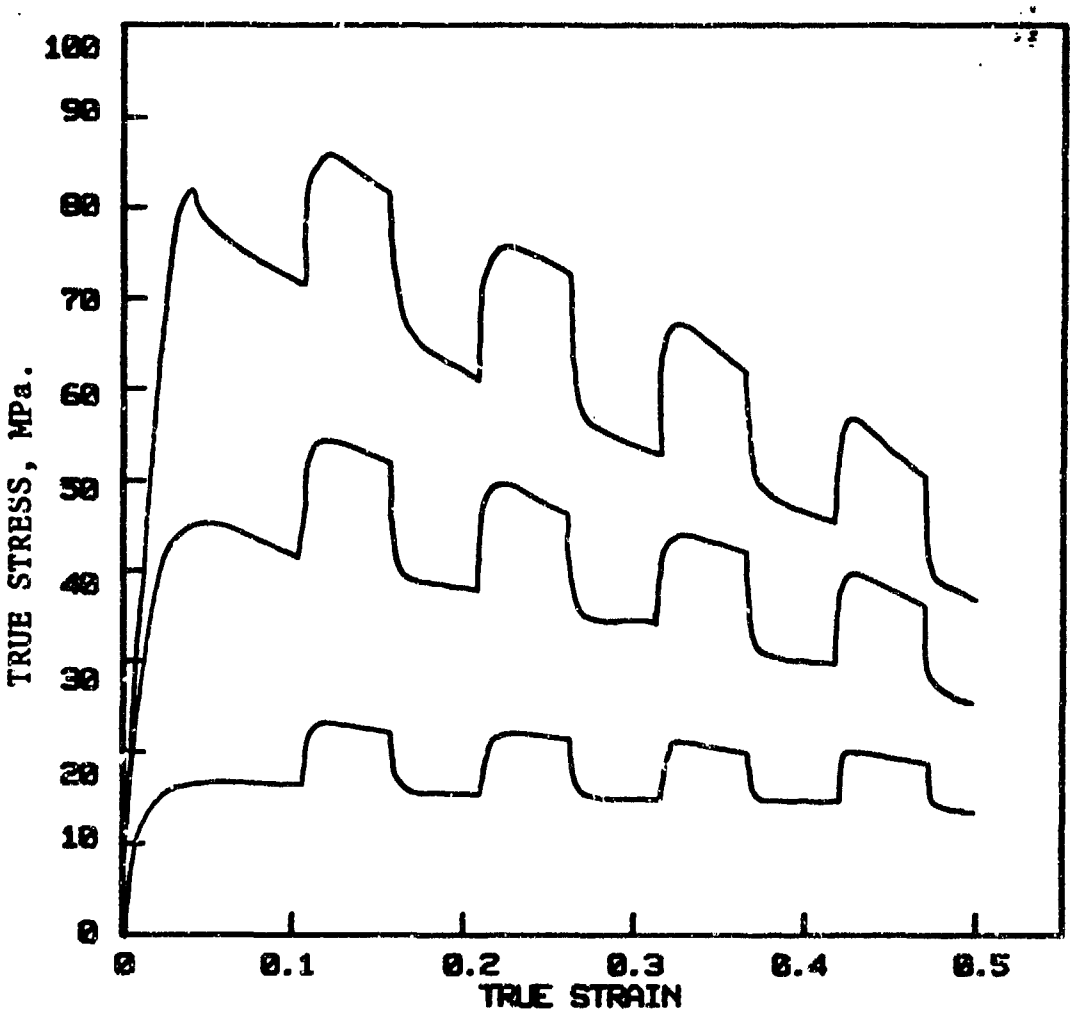

Figure 4. True stress–true strain curves from typical strain rate cycling tensile tests showing that the stress exponent, n , is independent of the overall strain hardening or strain softening behaviors.

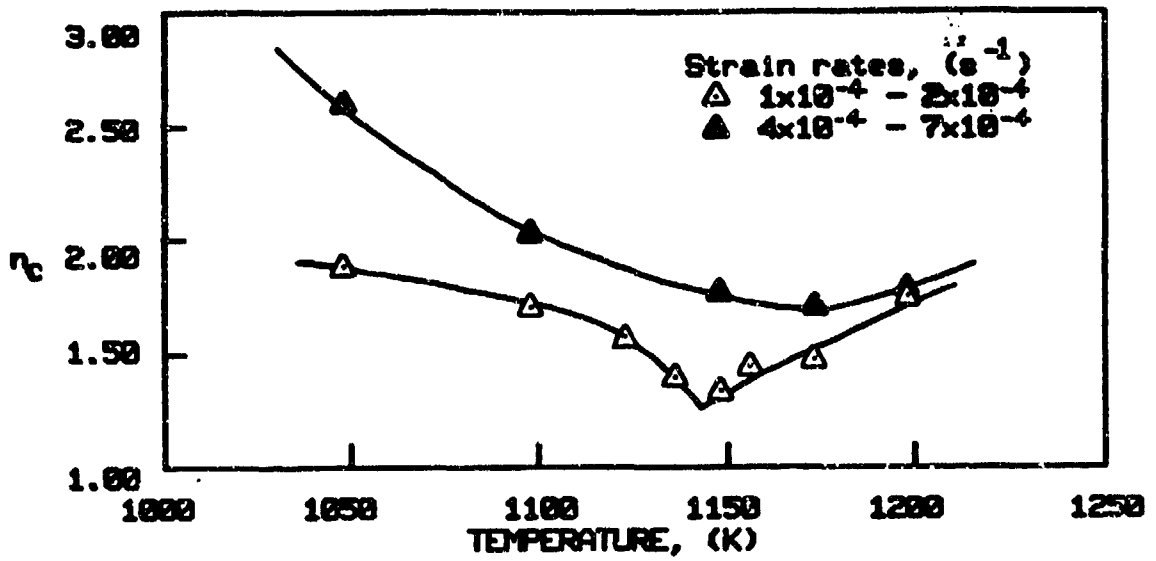

Figure 5a. Temperature dependence of the stress exponent, n_c, evaluated from the strain rate cycling tests.

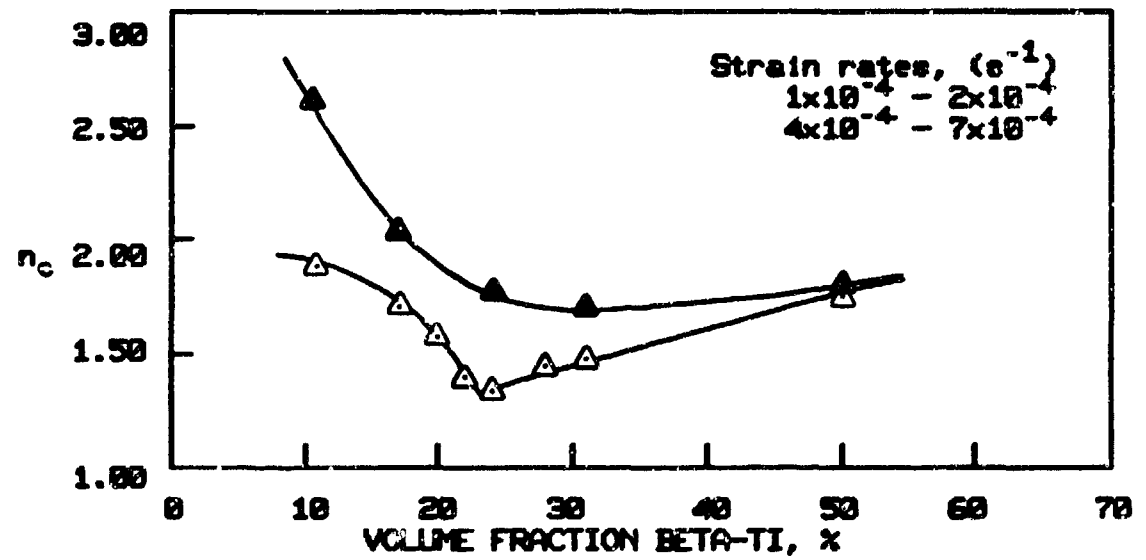

Figure 5b. Variation in the stress exponent, n_c (strain rate cycling tests), with volume fraction of beta-titanium.

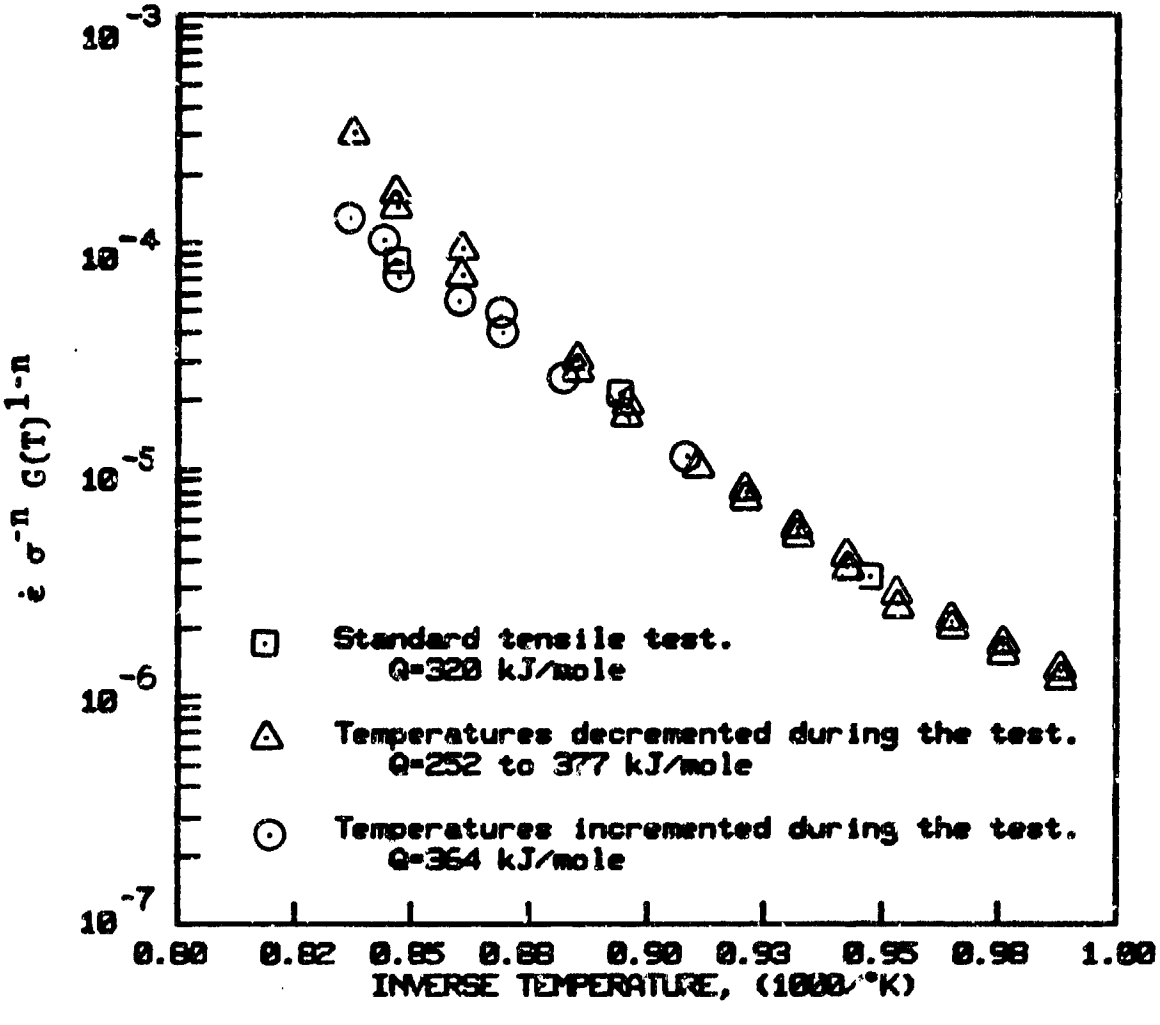

Figure 6. Results of both the standard uninterrupted tensile tests and tests where the temperature was periodically changed.

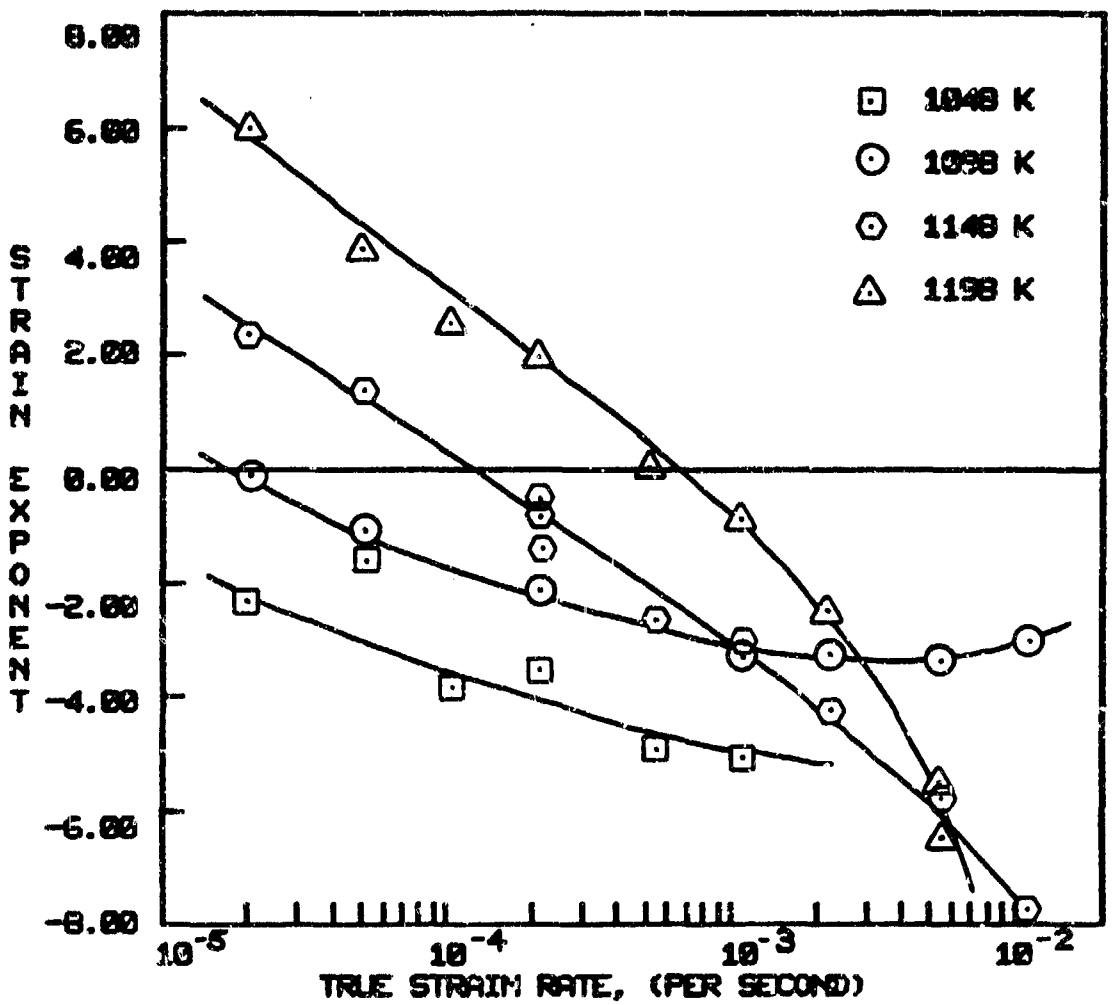

Figure 7. Strain exponent, h, as a function of true strain rate at different testing temperatures.

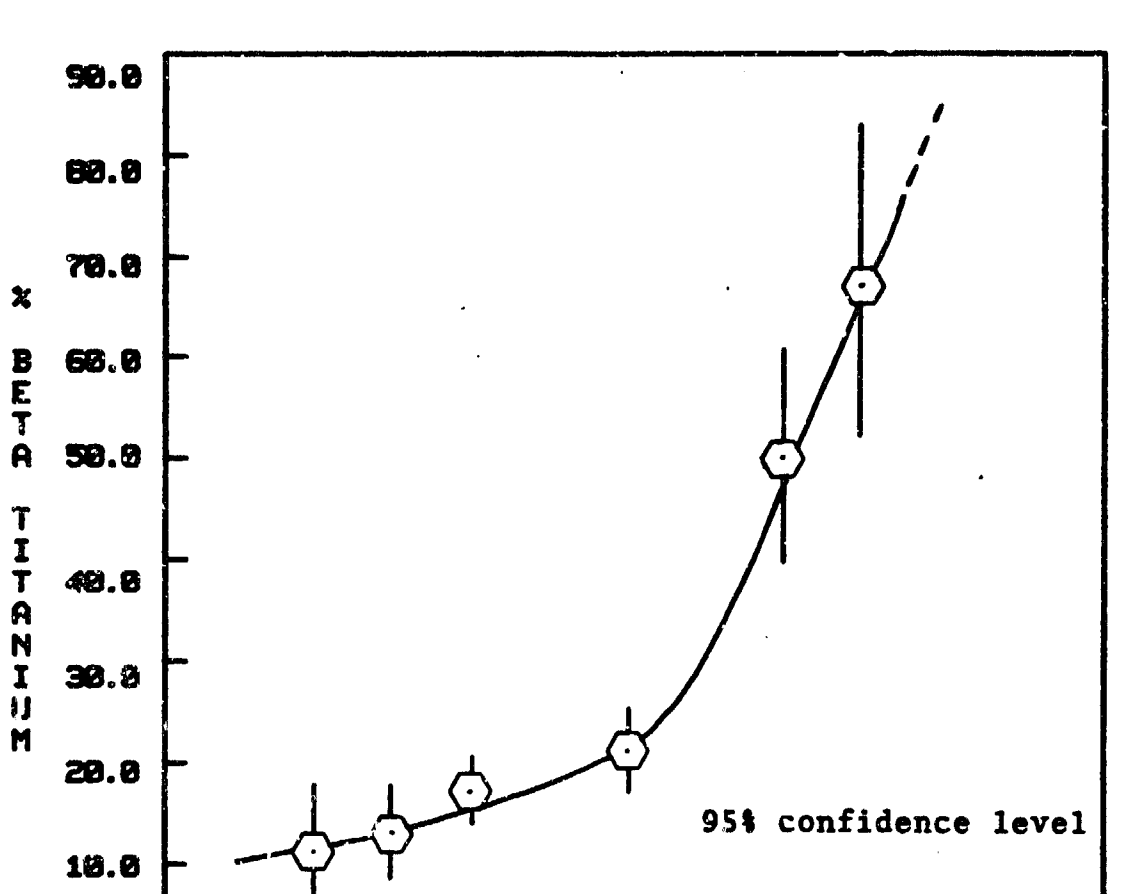

Figure 8. Equilibrium volume fraction of beta-titanium as a function of temperature.

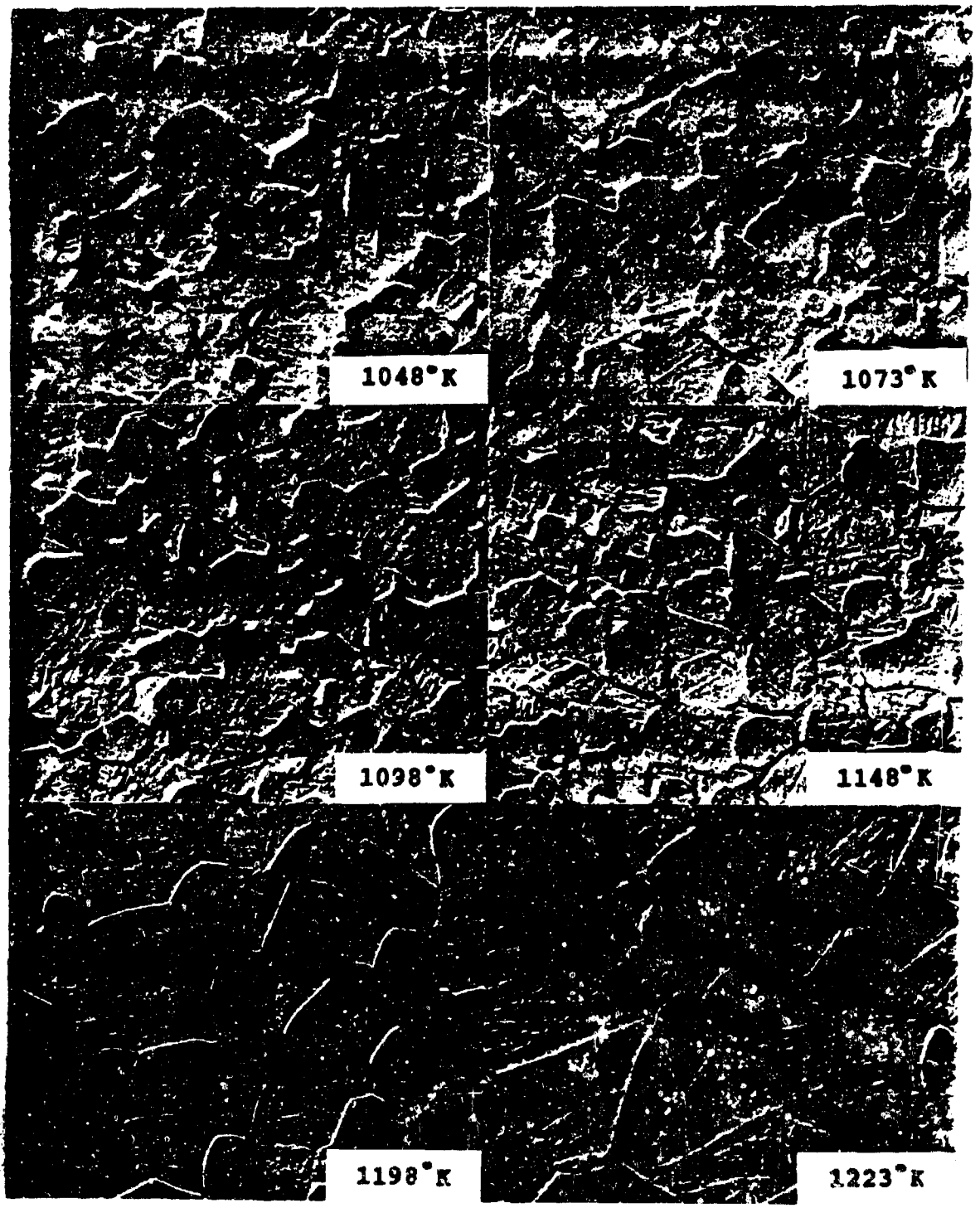

Figure 9. Microstructure of Ti-6Al-4V after annealing at various temperatures for 100 hours then water quenched.

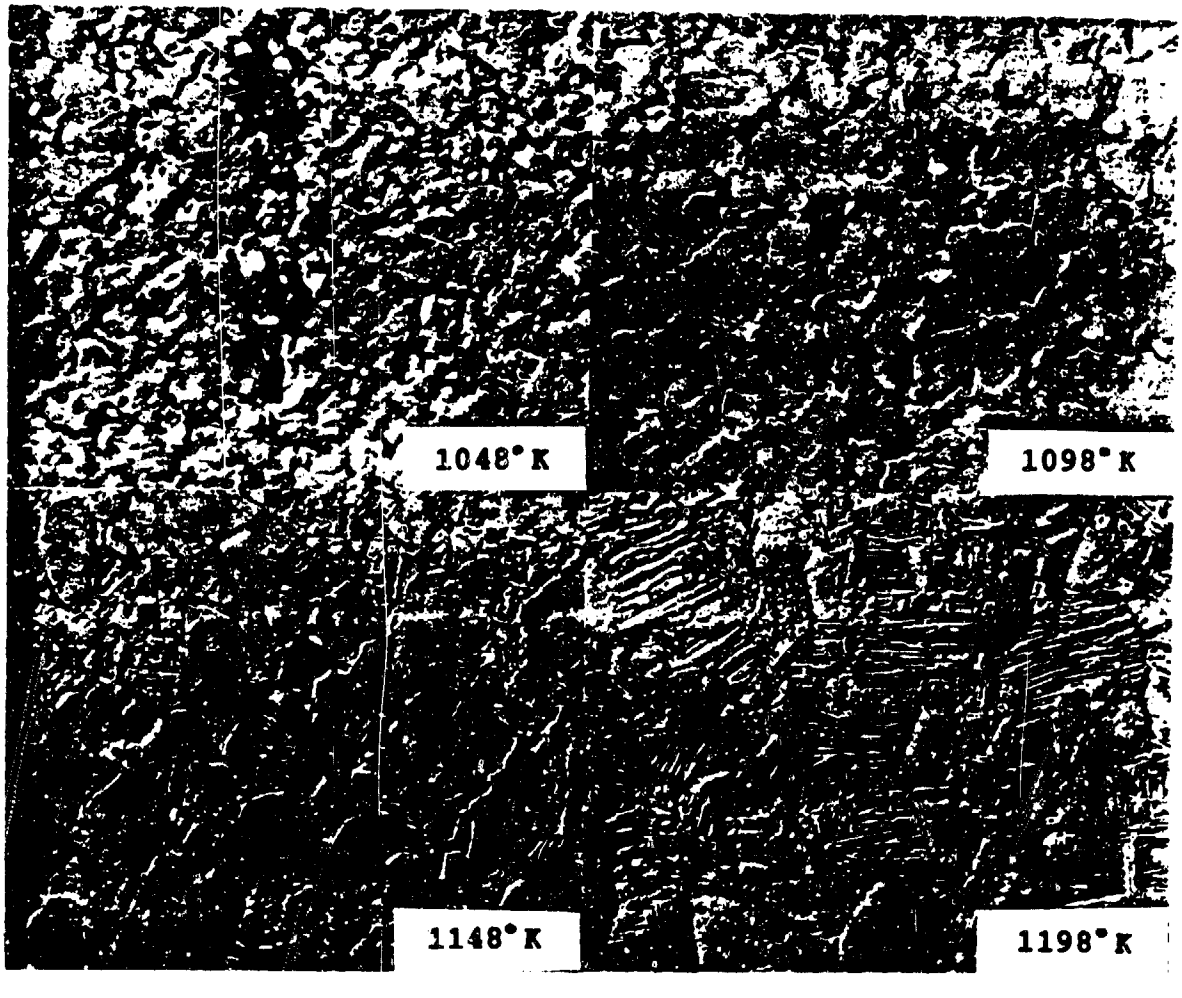

Figure 10. Microstructure of Ti-6Al-4V after tensile testing at a strain rate of 2×10^{-4} per second, true strain of 1.0 and different temperatures.

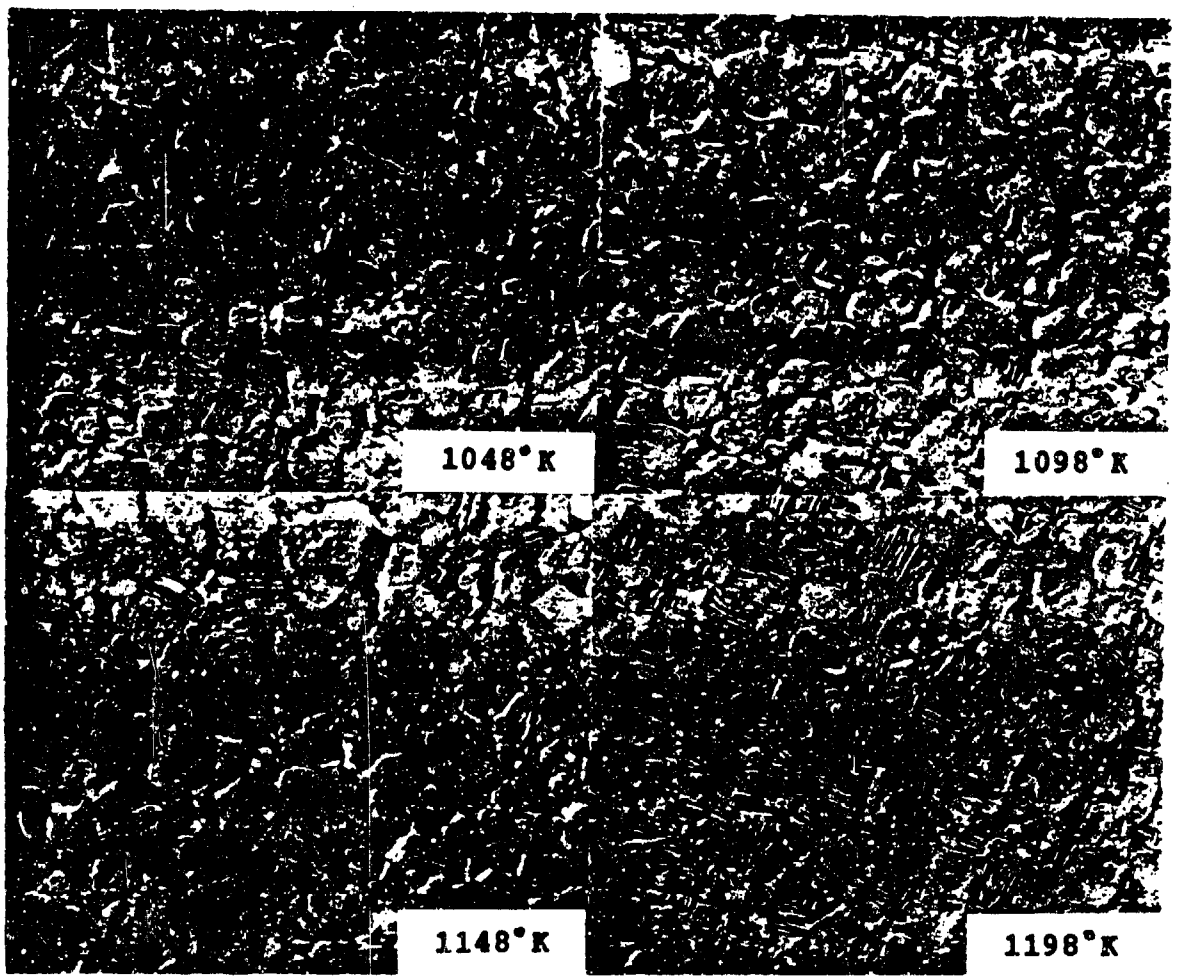

Figure 11. "Initial" microstructure of Ti-6Al-4V. Specimens show that the microstructure changes significantly during the brief time it takes for the furnace, grips and specimens to stabilize at the test temperature (twenty minutes at various temperatures).

SECTION 3

CORRELATION BETWEEN MECHANICAL PROPERTIES AND MICROSTRUCTURE IN A Ni-MODIFIED SUPERPLASTIC Ti-6Al-4V ALLOY

B. Hidalgo-Prada and A. K. Mukherjee

ABSTRACT

The superplastic deformation (SPD) properties of Ti-6Al-4V modified by the addition of 2 percent Ni (Ti-6Al-4V-2Ni) have been investigated in the temperature range between 750-870°C and strain rates from 10^{-5} - 10^{-2} s^{-1}. It was found that the effect of microstructural changes occuring during SPD produced strain hardening and strain softening. Metallographic evidence is presented to show that the observed strain hardening is due to deformation-enhanced grain growth of both α and β phases. The strain softening was primarily due to grain size refinement. Maximum attainable super-plastic ductility was found to be associated with a dynamic balance between strain hardening and softening. Wedging and pinching off of the α-grains by the more diffusable β-phase through grain boundary diffusion seems to be an important mechanism in the deformation process of the Ni-modified Ti-alloy in the superplastic temperature and strain-rate range studied.

INTRODUCTION

Many titanium alloys exhibit superplastic deformation behavior in the temperature range where the α and β phases co-exist. Ti-6Al-4V, the most commonly used Ti alloy, is superplastic at temperatures between 850°C and 950°C, with optimum superplastic properties attained near 925°C [1], the temperature frequently used for superplastic forming (SPF) operations with this alloy. However, lower SPF temperatures would be desirable to reduce oxidation problems, shorten forming cycle times, and reduce die costs. Thus, there is technological interest in lowering the forming temperature of Ti-6Al-4V by addition of a suitable β-stabilizer. Furthermore, alloy additions with high diffusivities can accelerate creep rates, allowing the creep process essential to superplastic deformation to proceed at reasonable rates below the conventional SPF temperatures for the base alloy. Alloy additions of β-stabilizers such as Ni, Fe, Co, that diffuse rapidly in Ti, have been found to lower the optimum SPF temperature of Ti-6Al-4V alloy [2,3]. Among these, Ti-6Al-4V alloy modified by the addition of 2 percent Ni (Ti-6Al-4V-2Ni) appears to possess the best potential in lowering the SPF

temperature without sacrificing the ease of its formability. This paper describes the work carried out to analize the superplastic deformation properties of the Ni-modified Ti-6Al-4V alloy and to correlate them to the microstructure. Furthermore, the mechanisms responsible for the observed stress-strain behavior in the Ti-6Al-4V-2Ni alloy and their correlation with the microstructural evolution produced by the deformation, are detailed.

EXPERIMENTAL PROCEDURES

The Ti-6Al-4V-2Ni alloy used in this investigation had a nominal composition (wt percent) of 5.78 Al, 0.08 Fe, 0.01 Co, 2.10 Ni and balance Ti. Original 7 kg ingots of the Ni-modified alloy (cast by TIMET) were broken down in the conventional manner, and finish-rolled in the $\alpha+\beta$ phase field to produce a fine mixture of equiaxed α and β grains. The final material was received as a sheet with thickness of approx. 1.3 mm, from which test specimens with tensile axis parallel to the rolling direction were machined. To optimize the initial microsturcture, tensile samples were annealed in purified argon atmosphere for 1 hour at 815°C.

Uniaxial tensile tests were conducted using an MTS servohydraulic machine interfaced with a PDP/11 computer and fast digital data acquisition system. A Quad Elliptical Radiant heating furnace provided a heating rate of 200°C/min, with a phaser power controller which maintained stable temperatures to within ±1°C. All tests were conducted in a purified argon atmosphere. Upon completion of the tests, specimens were quenched under load in pre-chilled argon. Samples were held at the test temperature for 20 minutes before testing.

To determine the SPD behavior pertinent to this investigation, two types of high temperature tests were conducted: 1) Continuous tensile tests to ascertain the effect of rate of deformation on the microstructural evolution, at constant temperature and for different strain levels up to fracture. 2) To minimize the effect of microstructural changes observed during SPD of the Ni-modified alloy, tensile specimens were pre-strained at temperature of 815°C and strain rate of 2×10^{-4} s^{-1} up to a total true strain of 0.20.

Samples from deformed specimens were investigated by scanning (SEM) as well as by transmission (TEM) electron microscopy.

RESULTS AND DISCUSSION

It has been determined that a large volume fraction of the β-phase in α-β titanium alloys, is essential to SPD [1]. Furthermore, it has been found that equal volume fraction of the two phases in a duplex alloy, produces optimum superplastic properties [4]. The static annealing of the Ni-modified $\alpha+\beta$ Ti at 815°C for 1 hour, (SA-1-815) produced volume fractions of the α-phase (f_α) and β-phase (f_β) approximately 1:1 (49 percent β). In addition, this heat treatment also yielded similar phase sizes (λ^α =

6.3 μm, λ^{β} = 5.7 μm). The main purpose of the annealing program was to obtain a suitable and similar initial microstructure for the tensile tests. Furthermore, contrary to earlier belief, it has been determined in previous work [5] as well as in the present investigation, that the microstructures of the base and Ni-modified alloys undergo substantial evolution during SPD. Thus, the concept of constant microstructure during deformation for this alloy becomes irrelevant. Instead, optimization of the initial microstructure for superplasticity is more desirable.

The temperature and strain rates selected for deformation in this investigation were such that the specimens deformed in region II of superplasticity. The results illustrated in Fig. 1, show the effect of the rate of deformation on the SPD behavior on the Ni-modified alloy. These test were conducted at high, intermediate and low strain rates (5 x 10^{-3}, 2 x 10^{-4}, 5 x 10^{-5} s^{-1}) for the optimum temperature of 815°C and up to true strain of 1.0. Fig. 1 also illustrates the processes of strain hardening and strain softening occurring during deformation. The strain softening observed at high strain rate

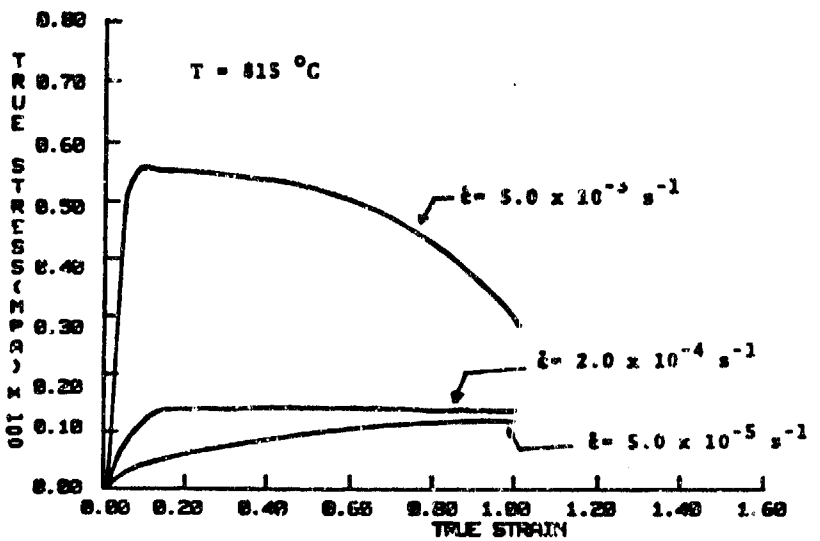

Fig. 1. Effect of strain rate on SPD behavior in Ti-6Al-4V-2Ni at optimum SPF temperature of 815°C and ε_T = 1.0.

Fig. 1. Effect of strain rate on SPD behavior in Ti-6Al-4V-2Ni at optimum SPF temperature of 815°C and ε_T = 1.0.

(5.0 x 10^{-3} s^{-1}), was primarily due to grain refinement of both α and β phases, as illustrated in Fig. 2. This process of grain refinement during SPD is due to dynamic recrystallization, which produces fine equiaxed new grains replacing the large grains. At low strain rates (5.0 x 10^{-5} s^{-1}), significant strain hardening effect was observed, as shown in Fig. 1.

Fig. 2. Dynamic Recrystallization process associated with strain softening during SPD in Ti-6Al-4V-2Ni, at T=815°C, $\dot{\varepsilon}$ = 5.0 x 10^{-3} s^{-1}, ε_T = 1.0.

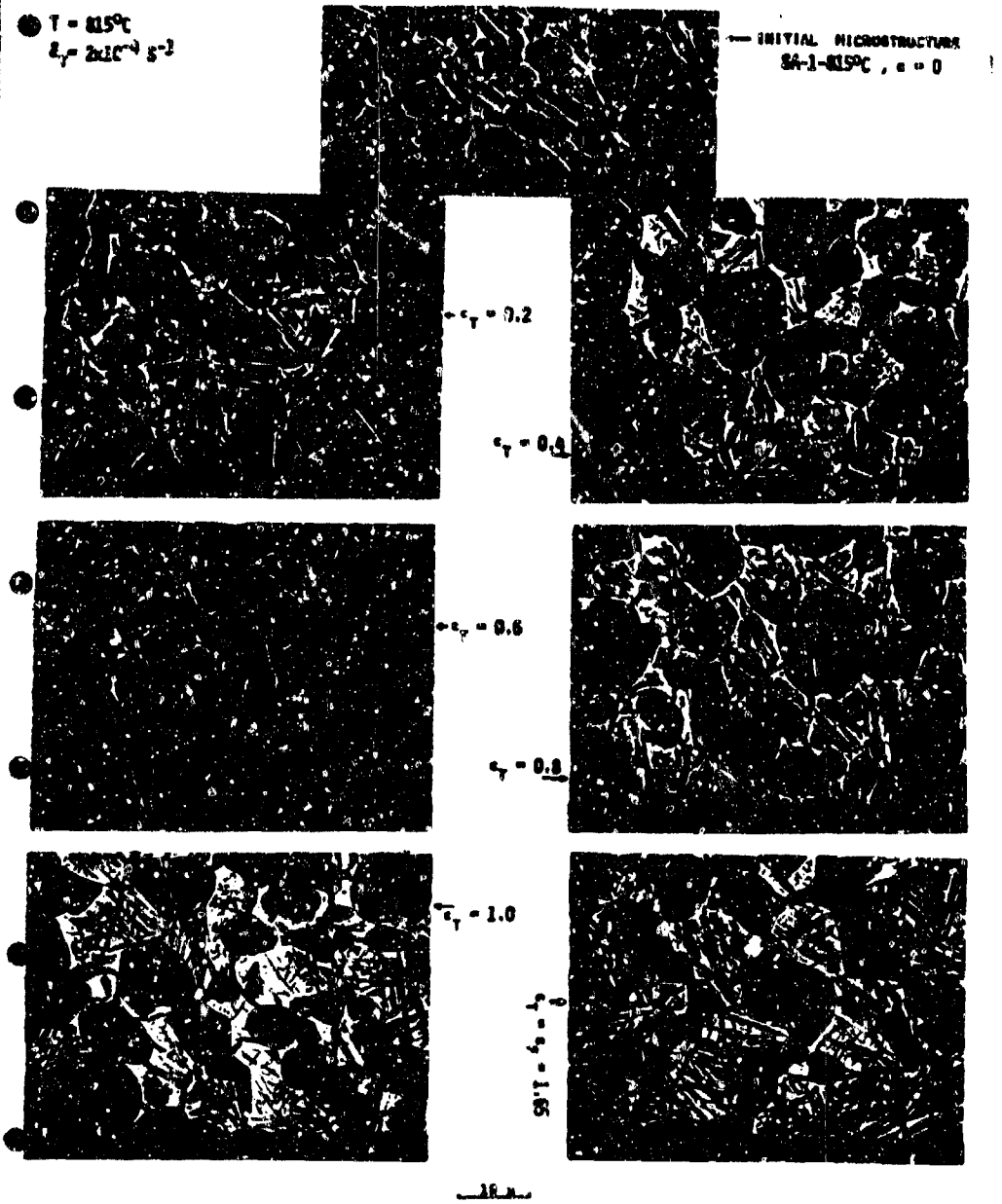

Fig. 3. Microstructural evolution as a function of strain showing the effect of deformation enhanced grain growth in Ti-6Al-4V-2Ni at constant, temperature and strain-rate.

Microstructural correlation is presented in Fig. 3. This micrograph shows that for test conditions leading to strain hardening, there is a deformation-enhanced growth of both α (dark) and β (light) phases. In the absence of overt cavitation, the maximum attainable superplastic ductility was associated with a dynamic balance between strain hardening (due to grain growth) and strain softening (due to recrystallization). This behavior was observed at intermediate strain rate (2.0×10^{-4} s^{-1}) as illustrated in Fig. 1.

For further characterization of the stress dependence of superplastic strain-rate, the true activation energy was calculated from pre-strained test samples deformed at constant strain rates of 2.0×10^{-4} and 5.0×10^{-4} s^{-1} and variable temperatures. Narrow temperature increments between 780°C (1053K) and 880°C (1153K) were used, to allow some degree of microstructural stability at each temperature and flow stress level. Furthermore, pre-strained specimens were used to obtain an activation energy value consistent with some degree of steady-state condition, with regard to the observed microstructural evolution. The average value of the true activation energy, Q_T, was found to be 145 KJ/mole. The activation energy for lattice self-diffusion Q_V, for the β-phase in Ti, obtained from radioactive ^{44}Ti tracer, have been found to be [6] about 248 KJ/mole. Thus, considering the activation energy for grain boundary diffusion, $Q_{GB} \approx 0.6\ Q_V$, we obtain $Q_{GB}(\beta\text{-Ti}) \approx 149$ KJ/mole, which is in good agreement with the $Q_T \approx 145$ KJ/mole determined. Hence, it appears that the true activation energy for SPD in the Ni-modified Ti alloy, is similar to that of grain boundary diffusion.

Previous investigations [2] on the mechanism for SPD in Ti-6Al-4V-2Ni, have suggested that the flow stress-strain rate behavior of each phase

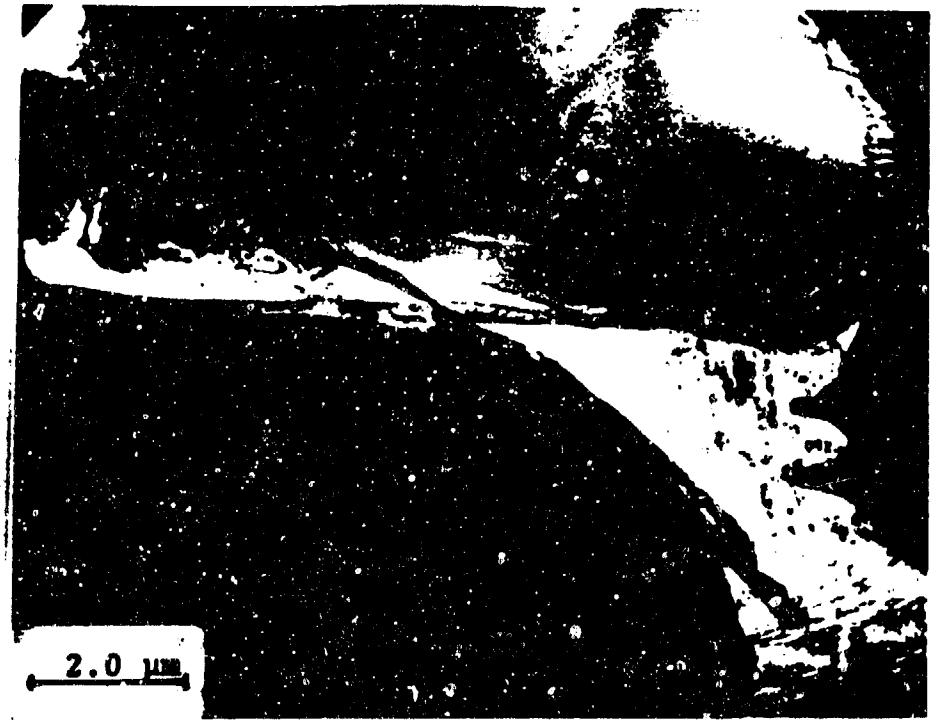

Fig. 4 Accomodation process during SPD in Ti-6Al-4V-2Ni, showing β-phase injection between α-phase grains. SA-1-815, $T = 815°C$, $\dot{\varepsilon} = 2.0 \times 10^{-4}\ s^{-1}$ $\varepsilon_T = 0.6$.

could be represented by the Ashby-Verrall model [7]. Our microstructural correlations of SPD behavior in the range of temperatures and strain-rates tested suggest otherwise. It appears that the controlling deformation process is that of interphase accomodation in agreement with the Spingarn-Nix model for deformation in two phase materials by diffusion creep [8]. As shown in Fig. 4, there is an apparent wedging and pinching off of the harder phase α by the more diffusible β-phase during the accomodation process. Furthermore, as predicted by the model, the interphase boundaries — appear to be curved — concave in the more diffusive β-phase, and convex in the harder phase α.

CONCLUSIONS

The superplastic deformation of Ti-6Al-4V-2Ni alloy deformed in region II showed strain hardening at low strain rates and strain softening at higher strain rates. The strain softening is primarily due to dynamic grain refinement. The strain hardening is due to deformation enhanced grain growth. Maximum attainable superplastic ductility was associated with a dynamic balance between hardening and softening behavior.

ACKNOWLEDGEMENT

The authors would like to acknowledge the encouragement of Dr. Alan Rosenstein of the Air Force Office for Scientific Research and the support from AFOSR 82-0081.

REFERENCES

1. N. E. Paton and C. H. Hamilton, Met. Trans., 10A, 241 (1979).
2. J. A. Wert and N. E. Paton, Met. Trans., 14A, 2535 (1983).
3. J. R. Leader, D. F. Neal and C. Hammond, Submitted for publication (1984).
4. D.M.R. Taplin and T. Chandra, J. Mat. Sci., 10, 1642 (1975).
5. G. Gurewitz, Ph.D. Thesis, University of California at Davis (1983).
6. J. F. Murdock, et al., Acta Metall., 12, 1033 (1964).
7. M. F. Ashby and R. A. Verrall, Acta Met., 21, 149 (1973).
8. J. R. Spingarn and W. D. Nix, Acta Met., 26, 13 (1978).

SECTION 4

SUPERPLASTIC DEFORMATION BEHAVIOR OF A FINE-GRAINED 7475 Al ALLOY

Mahidhara K. Rao and Amiya K. Mukherjee

SUMMARY

A commercial aluminium alloy, 7475 Al containing Fe, Si and Cr, and processed for fine grain size, was found to deform superplastically when tested at 457°C. The activation energy for superplastic flow is nearly equal to that for lattice diffusion and stress exponent is approximately equal to 2. It is suggested that lattice diffusion controls the deformation behavior at elevated temperature and the mechanism for plastic flow at 457°C is grain boundary sliding accomodated by slip processes occurring both within the grain and in the vicinity of the grain boundary. The microstructural features are compared with theoretical predictions of a model for superplasticity.

1. INTRODUCTION

Micrograin superplasticity, where relatively large neck free elongations can be obtained has been well documented in recent years [1,2]. Significant level of recent research effort has been directed towards the identification of the deformation mechanism(s) in superplastic alloys. Common superplastic alloys are usually of eutectic or eutectoid composition because both recrystallization and grain growth tend to be inhibited by chemical dissimilarity of the two phases [1,2]. However, if the grain size of an alloy remains fairly fine during deformation, owing to the presence of a small

amount of stable and dispersed second phase particles that stabilizes the grain size, then a nominally single-phase alloy could be superplastic when deformed at suitable strain-rates and temperature [3,4]. Hence there is some incentive in developing such nominally single phase superplastic alloys for practical use. There is also the need to study the rate controlling deformation mechanism for superplasticity in such alloys from a fundamental viewpoint.

Recent work by Wert, Paton, Hamilton and Mahoney [5] has indicated that grain-refinement in commercial 7000 series Al-Zn-Mg-Cu alloys (pseudo single phase alloy), is possible through thermomechanical treatments. An attractive feature of the type of treatment reported [5] is that conventional commercial alloys can be processed to a sufficiently fine grain size so that they become superplastic in their deformation behavior. The 7475 Al alloy with appropriate thermomechanical processing has emerged as a leading material for superplastic forming and has significant potential for structural applications [6-12]. However, few investigators have attempted a systematic study of the deformation mechanisms during high temperature flow of this alloy. Therefore, this investigation was undertaken in order to identify the deformation mechanism in this essentially single phase, fine grained 7475 Al alloy, having grain boundaries pinned by intermetallic particles.

2. EXPERIMENTAL PROCEDURE

The 7475 alloy has the chemical composition as shown in Table I. The alloy was obtained from ALCOA Research Laboratory after it was thermomechanically processed for fine grain size [5,13,14]. Tensile specimens with a gauge length of 7 mm and gauge width of 6.53 mm were cut from the as-received 2.53 mm sheet, in a direction parallel to the rolling direction.

These were then pre-annealed at 530°C for 24 hours in order to homogenize the microstructure.

The stress (σ)-strain rate ($\dot{\varepsilon}$) data were obtained over five orders of magnitude of strain-rate and in the temperature range 437-517°C using differential strain-rate tests. The test temperatures were controlled to an accuracy of ±1°C in all the tests by using a Quad Elliptical radiant furnace controlled by a phase power controller. All tests were performed in an argon atmosphere using a MTS 810 closed-loop servo-hydraulic test machine programmed to run in a constant strain-rate mode.

Metallographic examinations were conducted using optical and transmission electron microscopy. Samples were polished using the standard procedures and etched using Kellers reagent containing 4 ml HF, 6 ml HCl, 10 ml HNO_3 and 380 ml H_2O. Intercept lengths were measured by counting ~1000 grain boundary intercepts of the micrographs of longitudinal and transverse surfaces of the specimens. Here, the mean linear intercept length with an error bar of 95 pct confidence limit serves as a measure of grain size. From Fig. 1 the grain size of the annealed microstructure was ~14μm. Thin foils were prepared using a solution of 1:3 nitric acid: methanol, at minus 40°C and were examined in a Phillips EM400 transmission electron microscope operating at 100KV.

3. RESULTS

Grain-size measurements

Fig. 1 represents three dimensional optical, micrograph of the material after the pre-anneal of 530°C for 24 hours. It is clear from the above micrograph, that grain size and grain shape are not similar in the three mutually perpendicular sections. Detailed microstructural analysis has led to

the conclusion that the grain-size (mean linear intercept) in the elongated (rectangular parallelopiped) microstructures may be represented by the cube root of grain volume. In non-equiaxed microstructure the average of intercept lengths measured on the longitudinal and transverse surfaces (by drawing random lines) were comparable to the grain size estimated as a cube root of grain volume (15). Hence in the present investigation the latter parameter is used to represent the grain size. This approach was also adopted in a recent theoretical analysis [16] of the deformation behavior and also in experimental studies in Pb-Sn eutectic [17], and in microduplex stainless steel [18,19].

Mechanical Testing

The $\log(\sigma)$ vs $\log(\dot{\varepsilon})$ and m vs $\log(\dot{\varepsilon})$ curves determined from the tensile tests are shown in Fig. 2(a) and (b), respectively. Here m is the strain-rate sensitivity parameter, defined by $m = d(\log\sigma)/d(\log\dot{\varepsilon})$. The stress ($\sigma$) and strain-rate ($\dot{\varepsilon}$) relationship for lower test temperature of 437 and 457°C where low strain rate data are available, can be characterized by a sigmoidal curve. The strain-rate sensitivity parameter, m has a higher value in the intermediate range of strain-rates (Fig. 2b). The maximum value of m that was observed for each temperature decreased with decreasing temperature. Specimens were tested at various temperatures at an initial strain rate of 1×10^{-4} s^{-1}. Elongation increased with increasing temperature and neck-free elongations higher than 800 percent were possible at temperatures above 457°C. The elongation values for specimens tested at various strain rates at a temperature of 457°C are shown in Fig. 3. Maximum elongation of 840 percent was obtained at a strain rate of 1×10^{-4} s^{-1}. Thus it can be seen from Fig. 3 that, at 457°C, this material exhibits optimum superplastic ductility when deformed at a strain rate of 1×10^{-4} s^{-1}.

The true stress versus true strain curves for specimens deformed to a true strain of 1.4, at a preselected strain-rate of 1×10^{-4} s^{-1} and in the temperature range of 437-517°C, are shown in Fig. 4. It is clear from this figure that the material undergoes strain-hardening at all temperatures and the rate of strain-hardening increases with decreasing test temperatures. The effect of varying the strain-rate at a constant temperature is shown in Fig. 5. Here true stress-true strain curves (up to a true strain of 1.4) are plotted for the test conducted at 457°C and at various strain rates in the range $10^{-5} - 5 \times 10^{-3}$ s^{-1}. The rate of strain-hardening during the early part of deformation is found to increase with increasing strain-rates.

The activation energy (Q) at a constant strain-rate of 1×10^{-4} s^{-1} was determined from the usual steady-state creep equation [20]:

$$\dot{\varepsilon} = \frac{AD_o G b}{kT} \left(\frac{b}{d}\right)^p \left(\frac{\sigma}{G}\right)^n \exp\left(\frac{-Q}{RT}\right) \qquad (1)$$

where A is a dimensionless constant, $D_o \exp(-Q/RT)$ is the appropriate diffusion coefficient, Q the activation energy, G the shear modulus at test temperature, b the Burger's vector, p the grain size exponent and n=1/m, the stress exponent; k and R have their usual meanings. Constants for the constitutive equation used for the 7475 Al alloy are shown in Table II. The data shown in fig. 5 was used to obtain $\log(\sigma)$ vs $\log(\dot{\varepsilon})$ plots at various strain levels, as shown in fig. 6. The slope of the curves in Fig. 6 gives m, the strain-rate sensitivity. This strain rate sensitivity is shown, in Fig. 7a, as a function of strain-rate at various strain levels and in Fig. 7b, as a function of strain at various strain-rates. The parameter m reaches an approximate constant value of 0.5 beyond a true strain of 0.5, especially at a strain-rate of 1×10^{-4} s^{-1} of interest in the present study.

The activation energy was obtained from a plot of log ($\sigma^{-n}G^{n-1}T$) at constant $\dot{\varepsilon}$ against 1/T by using values for stress and appropriate values for n which is equal to 1/m, obtained from Fig. 7b. The strain dependence of the activation energy was investigated by using values for flow stress at different strain levels. From Fig. 8, the activation energy for superplastic flow Q, was calculated to be equal to 146 kJ/mole at a strain of 0.5, which is close to the activation energy for lattice diffusion in Al [23]. The experimentally measured activation energy increased to 172 kJ/mole and 166 kJ/mole, at strain levels of 0.7 and 1.0, respectively. The m, n and Q estimated from experimental data are summarized in Table III.

Metallography

Fig. 9 is a transmission electron micrograph of the annealed specimen depicting the pinning of the grain boundaries, by the chromium-rich particles which prevents the boundaries from migrating. In this alloy it was observed that the shape of the grains change during the superplastic flow. An investigation was made of the shape changes produced by superplastic deformation at strain-rate of 1×10^{-4} s^{-1} and temperature of 457°C. Fig. 10a, b and c represent optical micrographs along the three mutually perpendicular planes, LT (longitudinal), ST (short-transverse) and LS (longitudinal-transverse) respectively of a specimen which received a strain of 1.4. It is clear from these micrographs that due to deformation, grains change their shape along the three mutually perpendicular planes, i.e. from equiaxed to elongated along the LT (longitudinal) plane, remains elongated along the LS (longitudinal-transverse) plane and changes from a slightly elongated shape to equiaxed structure along the ST (short-transverse) plane.

Fig. 11a and b are transmission electron micrographs of specimens, that were deformed at a temperature of 457°C and at a strain-rate of 1×10^{-4} s^{-1} to strain level of 0.5 and 1.4, respectively. At 457°C, increase in superplastic strain is associated with increase in dislocation density. These dislocations are often observed and appear to have been emitted from grain-boundaries as shown in Fig. 12 and interact with chromium-rich particles inside the grain as shown in Fig. 13.

4. DISCUSSION

It is evident from Figs 4 and 5 that the 7475 alloy undergoes strain-hardening during superplastic deformation. Strain influences both the strain-rate sensitivity, m (shown in Figs. 7a and 7b), and activation energy for superplastic flow, Q (shown in Fig. 8). At a strain-rate of 1×10^{-4} s^{-1} the m value decreases from 0.7 to 0.5 (Fig. 7b) and remains virtually unchanged beyond true strain of 0.5. On the other hand, the activation energy, Q increases slightly beyond true strain of 0.5 from 146 KJ/mole to 166 KJ/mole. Nevertheless, these values for activation energy are close to that for lattice diffusion in Al-solid solution. Furthermore, the grain aspect ratio of the longitudinal grain size (d_L) to the longitudinal-transverse grain size (d_T), shown in Table IV, tends to increase considerably with strain due to the development of elongated grain structure without any significant change in the grain-size, under most of the test conditions. This grain elongation occurs along with an increase in the dislocation density (Figs. 11a and b). suggesting a significant level of deformation of grain interior. These dislocations are emitted from grain boundaries (Fig. 12) and interacts with Cr-rich particles in the matrix. This in turn influences the flow stress during superplasticity. In addition, some

of the matrix dislocations may be forced into a boundary to produce extrinsic dislocations. In Fig. 12, two sets of parallel extrinsic dislocations are present (arrowed). The absorption of crystal lattice dislocations by high angle grain boundary is described in terms of dissociation at a rate limited by climb, into grain boundary dislocations with burger's vector characteristic of the nature of the grain boundary [24]. The motion of such grain boundary dislocations in the plane of the boundary by concurrent glide and climb would give rise to grain boundary sliding.

Extensive interface (either grain or phase boundary) sliding is commonly observed during superplastic flow and the general trend is the same in every investigation: the contribution of grain boundary sliding (GBS) is maximum in region II and decreases at higher (region III) and lower (region I) strain-rates [2]. It has been found [25,26] that, grain boundary sliding, grain-switching process and grain rotation occur during deformation at maximum m in the Al-Zn-Mg alloy. It is often assumed implicitly that these processes can occur by grain boundary sliding with diffusional accomodation although the need for slip has been recognized by some [25,26]. Furthermore, Nix [27] argues that microscopic slip inside the grains will be necessary, in order to provide the internal torque, needed for grain rotation.

The present test results strongly suggest that true steady-state microstructure is never realized in this alloy and that dislocation activity takes place during superplastic deformation of the alloy at this temperature. Earlier literature [28] sometime mentions lack of dislocation activity, particularly in alloys that do not contain precipitates. Melton and Edington [29] pointed out that in these superplastic materials that do not contain precipitates, dislocations may completely traverse the grain without

encountering obstacles before being annhilated at the grain boundaries thereby producing less evidence for dislocation activity. Stress induced generation and motion of dislocations [30,31] would give rise to a microstructure that would change with imposed strain. This again is suggested to bring about elongation of the grains [32].

Hamilton et al. [7] were the first to study the deformation mechanism in the 7475 Al alloy. According to these investigators the Ashby-Verrall [33] model, which is based on grain boundary sliding accomodated by diffusional flow and dislocation creep, provides a good representation of the flow behavior of 7475 Al alloy at 516°C. However, it does not produce a good correlation of flow properties at lower temperatures, apparently because of the presence of intergranular precipitates, which form in increasing quantities as the temperature is reduced. Invoking the core and mantle concept of grain structure, Belzunce [34] reanalyzed the data of Hamilton et al. by considering the contribution from two independent creep mechanisms. One of these is due to grain boundary sliding accomodated by slip representing mantle deformation. This is based on the premise that, when activation energy for superplastic deformation is equal to that for lattice diffusion, the creep rate is inversely proportional to square of the grain size [35]. The other contribution [36] is due to creep representing core deformation. A detailed study of an Al-9Zn-1Mg alloy by Matsuki et al [26] has led to the conclusion that slip processes were occurring during grain boundary sliding. The concept of Sherby and Ruano [36] of GBS occurring in a mantle-like region adjacent to the grain-boundaries is considered similar to the "mantle-and-core" theory proposed by Gifkins [37]. According to Gifkins [37], each grain becomes effectively separated during superplasticity into non-deforming core

surrounded by mantle in which plastic flow occurs. Belzunce [34] reanalyzed the high temperature behavior [7] in 7475 Al alloy, using the core-mantle approach [36]. The experimental results agree quite favorably with the predictions of the analysis [36], particularly at the three lowest temperatures (371, 427 and 482°C). The correlation becomes poor at low strain rates ($<2 \times 10^{-3}$ s^{-1}) at 516°C. The lack of good correlations at 516°C (the commercial superplastic forming temperature) with respect to flow properties and m-value, is attributed to strain-hardening phenomenon in 7475 Al at this temperature. TEM studies further revealed that [34], the structure in the vicinity of the grain-boundary (mantle region) changes continually so as to make grain boundary sliding more difficult and promote strain hardening without the necessity of grain growth during superplastic deformation at 516°C. Thus the observation of TEM microstructure at 516°C supports the core-mantle concept of Gifkins [37], i.e., non-deformable core and a deformable mantle.

In the present study, grain size has remained virtually unchanged. The dislocation density has been found to increase both in the matrix and grain-boundary, with increasing strain levels. The increased dislocation density is responsible for the strain-hardening of the material as well as, the grain elongation that is observed. This observation is quite different from the one normally found in the literature [28] on superplastic alloys such as α/β brass, Pb-Sn eutectic, Al-Cu eutectic, Ti-6Al-4V, IN 744 stainless steel and Al-Ca alloy. In these alloys, strain-hardening is associated with grain growth and not to dislocation storage. This is expected since there are no precipitates to impede the motion of dislocations in the grain-interior. Dislocations generated on one part of the grain boundary traverse the grain

and are annihilated at another part of the grain boundary. Hence, no increase in the dislocation density occurs in the above mentioned alloy systems. In addition, the investigation of Hamilton et al. [7] on 7475 Al alloy, was conducted using specimens which was thermomechanically processed from a different heat. They were tested at a higher temperature. Hence these investigators observed less dislocation activity and more grain-growth in their specimens after testing. In the present study, both strain-hardening and grain elongation are related to the increase in the dislocation density shown in Figs. 11a and 11b.

Although, during the last decade, several detailed models have been proposed [38] for accomodation of grain boundary sliding at triple points by dislocation motion, which is rate controlling, these models suffer from several short coming. Some of these are:

(1) In models based on dislocation pile-ups the stress concentration of a dislocation array is calculated using the formula suggested by Eshelby et al. [39]. However, as pointed by Nix and Spigarn [40] the solution given by Eshelby et al. does not apply during climb of dislocation or during any other plastic deformation and a linear stress dependence for flow is obtained.

(2) The A value (eqn. 1) in each of these models is considered to be constant. However, "A" in eqn. 1 is by definition [20] a dimensionless quantity which incorporates all the microstructural details pertinent to the deformation mechanism, other than the grain size. Therefore, it seems unreasonable to expect all the materials exhibiting superplastic behavior or even samples of the same alloy which have received different thermomechanical treatments will possess the same microstructural characteristics and specifically the substructural details at the grain boundaries.

It is not intended here to compare our experimental results with the predictions of individual models for superplasticity. Instead, an attempt will be made to assess how the present results correlate with one specific model that puts some emphasis on the grain boundary substructure in the details of the accomodation process of grain boundary sliding. According to this model [41], strain is achieved, mainly by three dimensional grain-rearrangement which proceeds by interface sliding accompanied by migration and grain rotation. During the process, the boundary sweeps away solute atoms leaving behind a narrow zone which is cleaner and softer than the bulk of the grain. Under the action of the applied stress, and their own line tension the few pre-existing dislocations are attracted towards the moving boundary. Accomodation is achieved by the climb of individual dislocations, (without arranging themselves into a dislocation pile-up array) in a narrow region near the interfaces and annhilation into these interfaces. During the climb process, the dislocations multiply by a Bardeen-Herring mechanism [42] thus making the process self-regenerative. Due to the close proximity of the interfaces, the climb of individual dislocations will be controlled by the activation energy for grain boundary diffusion. At high stresses more dislocations will arrive at the interface from the grain interior. The critical step is the overcoming of the obstacles (particles) by the dislocations during their motion inside the grains by glide and climb process controlled by lattice diffusion. In addition dislocation motion within the grains may lead grain elongation as was observed in the present study. The model [41] predicts that the substructure parameter will not be a geometrical constant, but will vary with both interface structure and the structure of the narrow zone near the interface. According to this model activation energy for

superplasticity will correspond to that for grain boundary diffusion with a stress exponent, n equal to 2. The parameter A in Eqn. [1] will not be a constant. Gifkins [43] has criticized the important assumption that grain boundary migration coupled to grain boundary sliding varies with grain size for which he claims that there is no evidence.

In 7475 Al alloy the contribution to changes in structure parameter A in eqn. 1 would come from intragranular dislocation activity. However the average value of activation energy for superplastic deformation in this alloy was 161.76 kJ/mole which is close to that for lattice diffusion (142 kJ/mole) in Al-rich solid solution [23]. This value is different from the value for activation energy for grain bourdary diffusion obtained for Al-Zn-Mg alloy with Zr additions [25]. In this context, the activation energy for superplastic deformation of Al-Zn-Mg alloy with zirconium and chromium (Al-9.1Zn-0.89Mg-0.30Zr-0.09 wt. percent Cr) was approximately equal to that for lattice diffusion in Al-alloys i.e. 141.28 kJ/mole [23]. The addition of Cr causes E-phase ($Al_{18}Cr_2Mg_3$) to precipitate during thermal processing of the cast material [44]. The result provides evidence that the interaction of dislocations with E-phase particles contributed to the change in the activation energy from the value for grain-boundary diffusion to that for lattice diffusion in Al solid solution.

Furthermore, it has been found in Al-6wt. percent Mg containing Zr, Cr and Mn [44] that E-phase or (Mn, Cr) Al_7 - phase particles are present within the grains and that dislocations appeared to interact with such particle-types rich in chromium rather than with $ZrAl_3$ particles during deformation of this alloy. Conserva et al. [44] and Conserva and Leony [45] reported similar behavior in connection with the recrystallization of Al-Zn-Mg

and Al-Mg alloys containing Zr, Cr, and Mn, either singly or in combination. Probably when dislocations generated at grain boundary ledges or triple points traverse the grains to an opposite grain boundary, the climb of dislocations over Cr-rich particles takes place within the grains. Such a dislocation process is probably controlled by lattice diffusion in Al. In an Al-6 wt. percent Mg containing Cr and Zr, it is suggested [46] that dislocation interacts more strongly with irregularly shaped Cr rich particles than with $ZrAl_3$ particles. Thereforе, it seems reasonable to assume that grain boundary sliding, and hence superplastic deformation of this alloy, is controlled by dislocation climb over the Cr-rich precipitate particles in the grain interior.

In 7475 Al, thermomechanical processing results in two types of hard intermetallic particles, due to the presence of 0.10 max. wt percent Si, 0.12 max wt. percent Fe and 0.18-0.25 wt. percent Cr: (a) Cr-rich particles and (b) Impurity (Fe and Si) rich particles. The dislocation substructure in this alloy, particularly at higher strain consists of predominantly dense tangles of fairly homogenously distributed dislocations (Fig. 11b) that show little tendency for being confined to well defined slip planes. The formation of such dislocation tangles clearly reflects the ability of the dislocations to readily climb away from obstacles. An examination of the substructure shows that the presence of non-shearable particles present in the microstructure promotes the formation of dislocation entanglements. The interaction of dislocations with the Cr-rich dispersoids leads to a dense tangle around each particle, which acts as an effective barrier to dislocation motion. The dislocations have to bypass these barriers by climbing over them.

In a fashion similar to that in Al-Zn-Mg and Al-Mg alloy, the superplastic flow in 7475 Al alloy is suggested here to be controlled by dislocation climb over the Cr-rich precipitate particles in the grain interior. These dislocations eventually reach the grain boundary where they climb into the boundary and are annhilated. However, in these sequential processes, the rate is controlled by the slower process of the climb motion of the dislocations over the Cr-rich particles. Hence the activation energy of the superplastic deformation will correspond to that for lattice diffusion. The important constitutive parameters n and Q_c determined at various strain levels, as summarized in Table 3, are similar to that determined in an earlier study [34]. However, the rate controlling mechanism of plastic flow in the present work is suggested to be grain boundary sliding accomodated by climb-glide processes occurring both within the grain and close to the grain-boundary.

5. CONCLUSION

1. 7475 Al alloy containing Fe, Si and Cr can deform superplastically at 457°C, and grain boundary sliding accompanied by dislocation motion within the grains is likely to be the predominant mode of deformation during superplastic flow of this alloy.

2. During superplasticity the grains elongate and dislocations interact with precipitate particles within the grains at 457°C.

3. The activation energy for superplastic flow, Q is close to that lattice diffusion in this alloy and the stress exponent, n is close to 2.

4. The microstructural features in 7475 Al alloy at 457°C are correlated with the predictions of a model due to Arieli and Mukherjee [41].

ACKNOWLEDGEMENT

This work is supported by the U.S Air Force Office for Scientific Research. The encouragement of Dr. Alan Rosenstein is appreciated.

REFERENCES

1. R. H. Johnson, Metallurgical Rev., 15 (1970) 115.

2. K. A. Padmanabhan and G. J. Davies, in "Superplasticity," Springer-Verlag Berlin Heidelberg, New York, 1980.

3. H. E. Cline and T. H. Alden, Trans Met. Soc. AIME, 239 (1967) 710.

4. N. Ujiiye, Mat. Sci. J. Japan, 6 (1969) 182.

5. J. A. Wert, N. E. Paton, C. H. Hamilton and M. W. Mahoney, Met. Trans., 12A (1981) 1265.

6. N. E. Paton, J. A. Wert, C. H. Hamilton and M. W. Mahoney, J. of Metals, 34 (1982) 21.

7. C. H. Hamilton, C. C. Bampton and N. E. Paton, in N. E. Paton and C. H. Hamilton (editors), "Superplastic Forming of Structural Alloys," Metallurgical Society of AIME, 1982, p. 173.

8. C. C. Bampton and J. W. Edington, Met. Trans., 13A. (1982) 1721.

9. C. C. Bampton and R. Raj, Acta Met., 30 (1982) 204.

10. C. C. Bampton and J. W. Edington, J. Engr. Mater. and Tech., 105 (1983) 55.

11. C. C. Bampton, M. W. Mahoney, C. H. Hamilton, C. H. Hamilton, A. K. Ghosh and R. Raj, Met. Trans., 14A (1983) 1583.

12. M. W. Mahoney, C. H. Hamilton and A. K. Ghosh, Met. Trans., 14A (1983) 1593.

13. N. E. Paton and C. H. Hamilton, "Method of Imparting a Fine Grain Structure to Aluminium Alloys Having Precipitating" Constituent U.S. Patent 4,092,181 (1978).

14. C. H. Hamilton, M. W. Mahoney and N. E. Paton, "Method of Imparting a Fine Grain Structure to Aluminium Alloys Having Precipitating" Constituent U.S. Patent 4,222,797, (1980).

15. F. Schucker, in "Quantitative Microscopy" McGraw-Hill Book Company, New York, (1968) 201.

16. W. D. Nix, Metals Forum, 4 (1981) 38.

17. B. P. Kashyap and G. S. Murty, J. Mat. Sci., 18 (1983) 2063.

18. B. P. Kashyap and A. K. Mukherjee, in J. B. Bilde-Sorensen et al. (editors), Proc. of 4th Intl. Symp. on "Deformation of Multi-Phase and Particle Containing Materials," , Riso National Laboratory, Roskilde, Denmark, 1983, p. 325.

19. B. P. Kashyap and A. K. Mukherjee, in B. Wilshire and D.R.J. Owens (editors), Proc. 2nd Intl. Conf. on Creep and Fracture of Engineering Materials and Structures, Swansea, 1984 p. 185.

20. A. K. Mukherjee, J. E. Bird and J. E. Dorn, Trans. Am. Soc. Metals, 62 (1969) 155.

21. Handbook of Physics and Chemistry, 53rd Edition, CRC Press, Cleveland OH, 1972-73, p. F-48.

22. G. Simmons and H. Wang, Single Crystal Elastic Constant and Calculated Aggregate Properties, Cambridge, Massachussets, MIT Press, 1971.

23. T. S. Lundy and J. F. Murdock, J. Appl. Phys. 33 (1968) 1671.

24. R. C. Pond and D. A. Smith, Phil. Mag. 36A (1977) 353.

25. K. Matsuki, Y. Ueno and M. Yamada, J. Japan Inst. Metals, 38 (1974) 219.

26. K. Matsuki, H. Morita, M. Yamaoa and Y. Murakami, Metal Sci., 11 (1977) 156.

27. W. D. Nix, in S. Agrawal (editor), 1984 ASM Superplastic Forming Symposium, Los Angeles, CA, 1964, p. 3.

28. B. P. Kashyap and A. K. Mukherjee, in "Overview: Microstructural aspects of Superplasticity" to be published in Journal of Materials Science.

29. K. N. Melton and J. W. Edington, J. Inst. Metals, 7 (1973) 172.

30. O. A. Kabyshev, B. V. Rodionov and R. Z. Valiev, Acta Met., 26 (1978) 1877.

31. L. E. Murr, "Interfacial Phenomena in Metals and Alloys," Addison-Wesley Publishing Co., Massachussets, (1975) 338.

32. P. Chaudhari, Acta Met., 15 (1967) 1777.

33. M. F. Ashby and R. A. Verrall, Acta Met., 21 (1973) 149.

34. J. M. Belzunce in "Superplasticity of Fine-Grained Aluminium Alloys," Engineer Thesis, Stanford Univ., (1983).

35. H. W. Hayden and J. H. Brophy, Met. Trans., 8A (1977) 1951.

36. O. D. Sherby and O. A. Ruano in N. E. Paton and C. H. Hamilton (editors), "Superplastic Forming of Structural Alloys," Met. Soc. of AIME, 1982, p. 241.

37. R. C. Gifkins, Met. Trans., 7A (1976) 1225.

38. A. Arieli and A. K. Mukherjee, Met. Trans., 13A (1982) 717.

39. J. D. Eshelby, F. C. Frank and F. R. N. Nabarro, Phil. Mag. 42 (1951) 351.

40. J. R. Spigarn and W. D. Nix, Acta Met., 27 (1979) 171.

41. A. Arieli and A. K. Mukherjee, Mat. Sci. Engr. 45 (1980) 61.

42. J. Bardeen and C. Herring, in W. Shockley (editor), "Imperfections in Nearly Perfect Crystals, J. Wiley, New York, N.Y., 1952, p. 279.

43. R. C. Gifkins in N. E. Paton and C. H. Hamilton (editors), Superplastic Forming of Structural Alloys, Met. Soc. of AIME, 1982 p. 3.

44. M. Conserva, E. DiRusso and O. Caloni, Met. Trans. 2 (1971) 1227.

45. M. Conserva and M. Leoni, Met. Trans., 6A (1975) 189.

46. K. Matsuki, Y. Uetani, M. Yamada and Y. Mura Kami, Met Sci., 10 (1976) 235.

TABLE I

Composition Limits of the 7475 Al alloy used.

Si	Fe	Cu	Mn	Mg	Cr	Zn
0.10 max.	0.12 max	1.2 to 1.9	0.6 max	1.9 to 2.6	0.18 to 0.25	5.2 to 6.

Ti	Other, Each	Others, total	Al
0.06 max	0.05 max	0.15 max	Remainder

TABLE II

Constants for the constitutive equation used for the 7475 Al alloy

Symbol	Name	Constant	Reference
D_o	Diffusion Coefficient	1.71 $cm^2\ s^{-1}$	21
b	Burgers vector	2.8×10^{-8} cm	21
k	Boltzmann's constant	$1.38 \times 10^{-23} JK^{-1}$	general
R	Universal gas constant	8.314 J $mole^{-1}k$	general
G	Shear modulus (MPa)	2.0×10^4 (at 710K)	22
		1.96×10^4 (730K)	22
		1.92×10^4 (750K)	22
		1.87×10^4 (770K)	22
		1.83×10^4 (790K)	22

TABLE III

The variation of parameters m, n and Q with superplastic strain

Parameter	$\epsilon = 0.5$	$\epsilon = 0.7$	$\epsilon = 1.0$
m (from Fig. 7b)	0.549	0.531	0.520
n	1.82	1.88	1.92
Q (kJ $mole^{-1}$)	146.	172.	166.

TABLE IV

Summary of grain-size measurements

CONDITION	$\bar{d}$	d*	AR	d_L	d_T	d_S
ANNEALED	14.19	13.76	1.155	17.81	15.41	10.29
$\dot{\varepsilon}=1x10^{-4}s^{-1}$, $\varepsilon=1.4$, T=437°C	10.14	9.46	1.65	14.95	9.05	6.042
$\dot{\varepsilon}=1x10^{-4}s^{-1}$, $\varepsilon=1.4$, T=457°C	12.16	14.40	1.44	22.47	15.63	9.230
$\dot{\varepsilon}=1x10^{-4}s^{-1}$, $\varepsilon=1.4$, T=497°C	14.14	15.82	1.43	24.04	16.81	10.66
$\dot{\varepsilon}=1x10^{-4}s^{-1}$, $\varepsilon=1.4$, T=517°C	15.19	18.12	1.41	24.73	17.53	14.99
$\varepsilon=1.4$, T=457°C, $\dot{\varepsilon}=1x10^{-5}s^{-1}$	14.20	15.01	1.41	19.19	13.60	14.13
$\varepsilon=1.4$, T=457°C, $\dot{\varepsilon}=5x10^{-5}s^{-1}$	13.74	14.72	1.40	22.00	15.71	10.00
$\varepsilon=1.4$, T=457°C, $\dot{\varepsilon}=1x10^{-4}$	14.14	14.40	1.44	22.47	15.63	9.23
$\varepsilon=1.4$, T=457°C, $\dot{\varepsilon}=5x10^{-3}$	13.05	14.04	1.94	24.43	12.58	9.00
T=457°C, $\dot{\varepsilon}=1x10^{-4}s^{-1}$, $\varepsilon=0.3$	13.90	13.79	1.24	17.47	14.08	11.56
T=457°C, $\dot{\varepsilon}=1x10^{-4}s^{-1}$, $\varepsilon=0.5$	12.15	13.71	1.28	18.00	14.00	10.20
T=457°C, $\dot{\varepsilon}=1x10^{-4}s^{-1}$, $\varepsilon=0.7$	12.50	13.78	1.31	18.20	13.82	10.40
T=457°C, $\dot{\varepsilon}=1x10^{-4}s^{-1}$, $\varepsilon=1.0$	12.65	14.40	1.44	19.90	13.63	10.00
T=457°C, $\dot{\varepsilon}=1x10^{-4}s^{-1}$, $\varepsilon=1.4$	14.14	14.40	1.44	22.47	15.63	9.23
T=457°C, $\dot{\varepsilon}=1x10^{-4}s^{-1}$, $\varepsilon=2.24$	11.85	15.70	2.03	29.95	14.69	8.79

Nomenclature used:

d_L = mean grain-size in the longitudinal direction (on the LT plane)

d_T = mean grain-size in the longitudinal-transverse direction (on the LT plane)

d_S = mean grain-size in the short-transverse direction (on the ST plane)

AR = Aspect Ratio = d_L/d_T

d* = $(d_L \times d_T \times d_S)1/3$

$\bar{d}$ = average of the mean grain sizes in the three mutually perpendicular sections ($=d_L+d_T+d_S/3$)

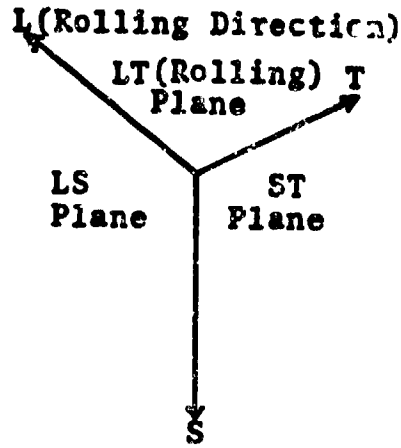

Fig. 1. Optical micrograph of the 7475 Al alloy annealed for 24 hours at 530°C. In the figure, the symbols L, T and S indicate longitudinal (rolling) direction, L, on the LT (rolling) plane, longitudinal-transverse direction on the LT (rolling) plane and short-transverse direction on the ST (short transverse) plane, respectively.

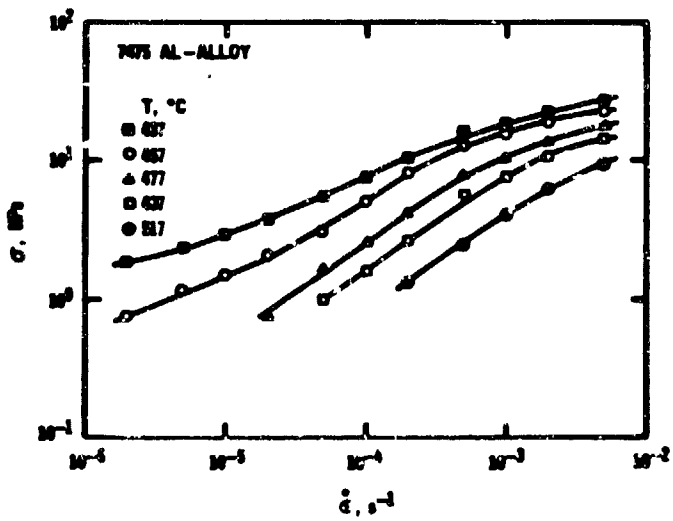

Fig. 2a. True stress-true strain rate behavior at various temperatures for the alloy using differential strain-rate test technique.

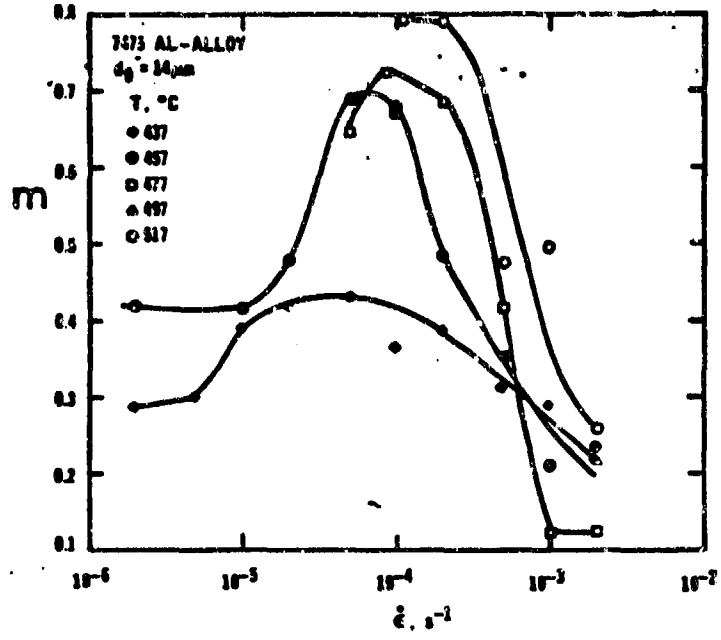

Fig. 2b Strain-rate sensitivity versus strain-rate at various temperatures for the alloy, obtained from Fig. 2a.

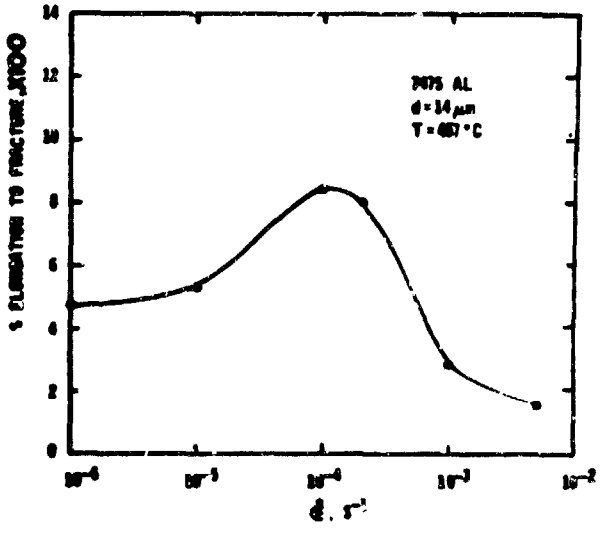

Fig. 3. Percentage elongation to fracture at various strain-rates for the alloy.

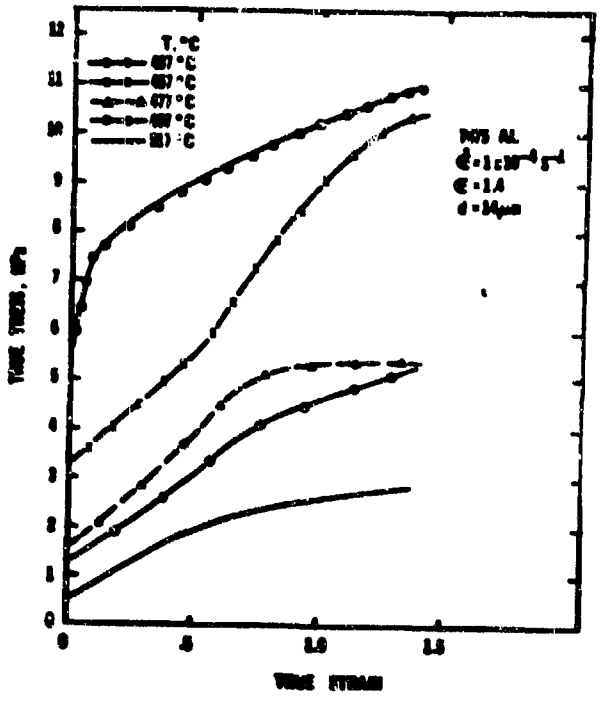

Fig. 4. True stress-true strain curves obtained, by keeping all parameters the same but changing only temperature.

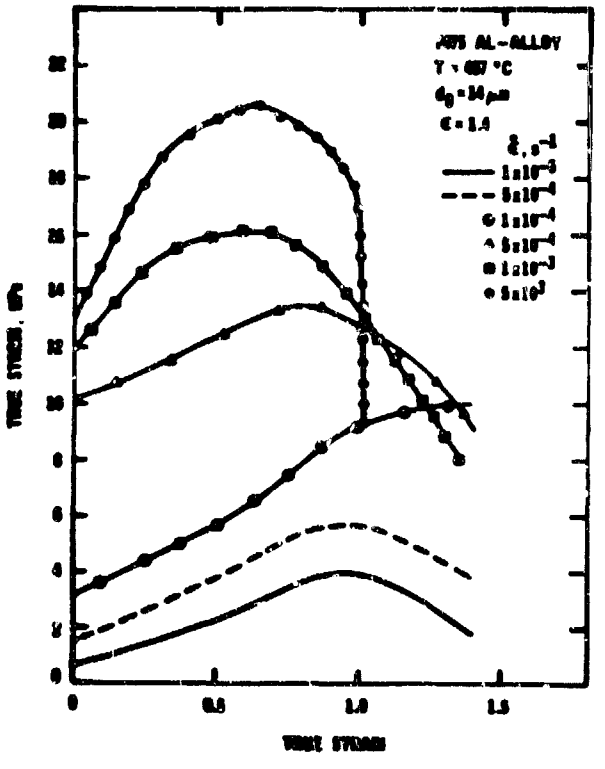

Fig. 5. True stress-true strain curves optained by keeping all parameters the same but changing only strain-rate.

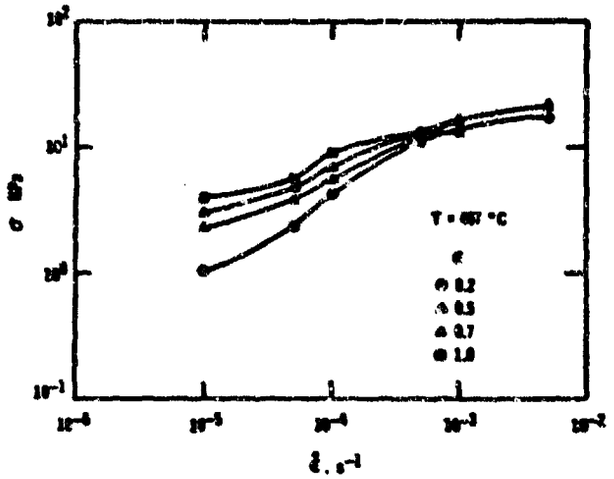

Fig. 6 True stress-true strain rate behavior at various strain levels obtained from Fig. 5.

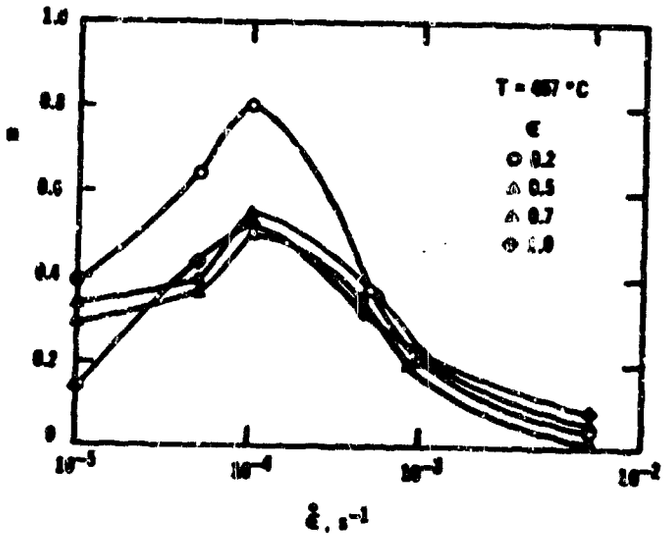

Fig. 7a. Strain rate sensitivity versus true strain-rate at various levles of true strain obtained from Fig. 6.

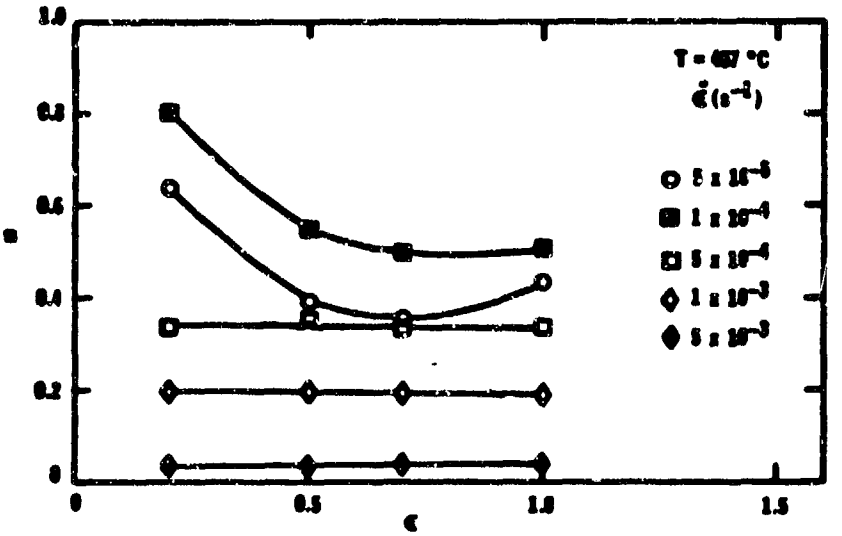

Fig. 7b. Strain-rate sensitivity versus true strain at various strain rates obtained from Fig. 6.

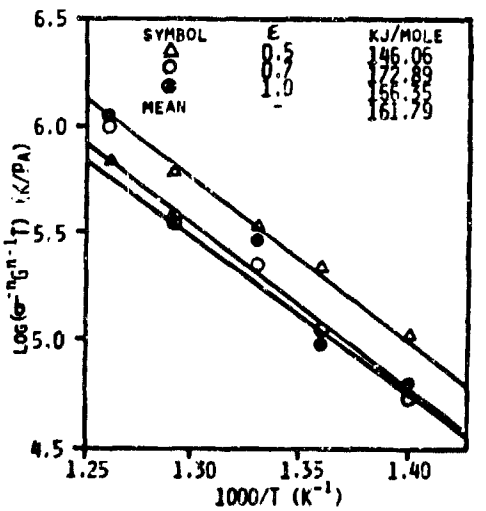

Fig. 8. Activation energy plot in Region II for the 7475 Al alloy.

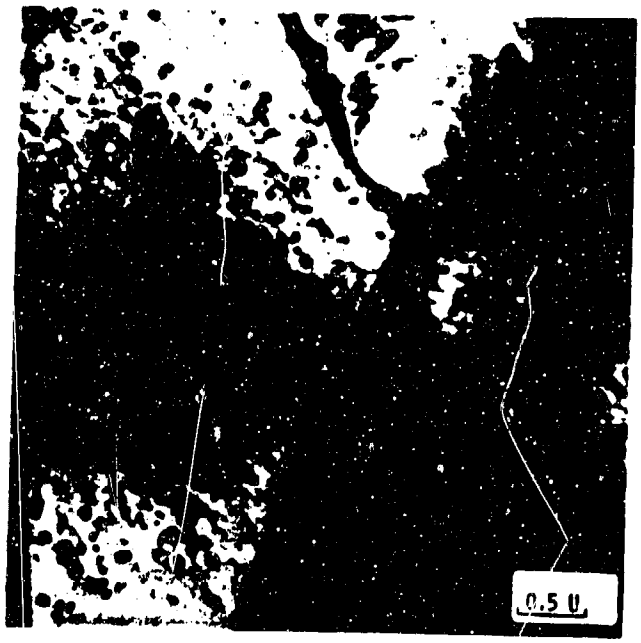

Fig. 9. Transmission electron micrograph showing grain-boundary pinning by intermetallic particles.

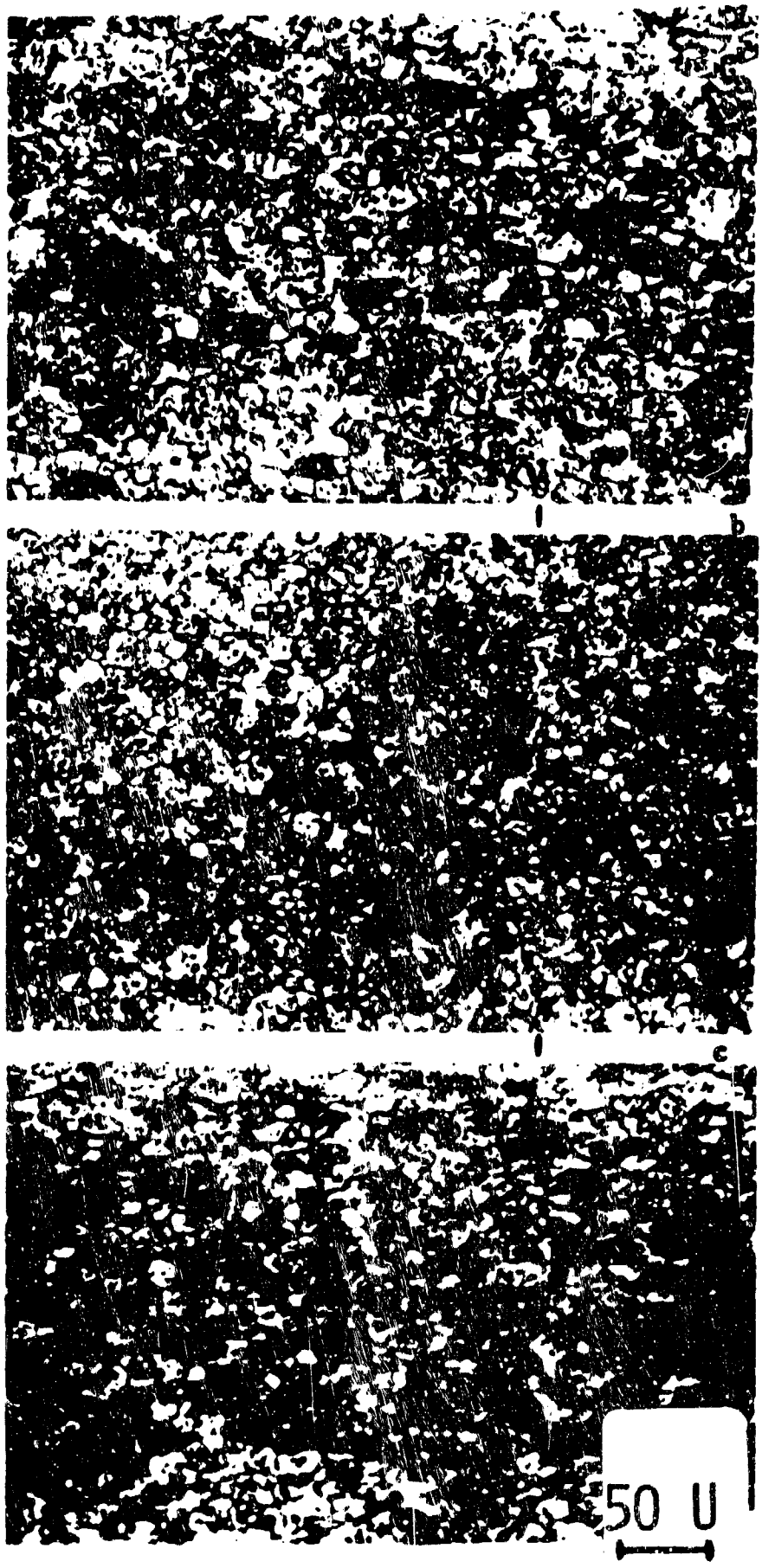

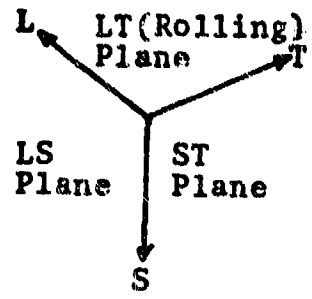

(a)

(b)

(c)

Fig. 10. Optical micrograph of the 7475 Al alloy deformed at a strain-rate of 1×10^{-4} s^{-1} and temperature of 457°C to a true strain of 1.4 taken along:
(a) LT (longitudinal, rolling) plane
(b) (ST) transverse) plane
(c) (longitudinal-transverse) plane.

(a)

(b)

Fig. 11. Transmission electron micrographs of a 7475 Al alloy, deformed, at strain-rate of 10^{-4} s^{-1} and temperature of 457°C to, strain levels of (a) 0.5 and (b) 1.4.

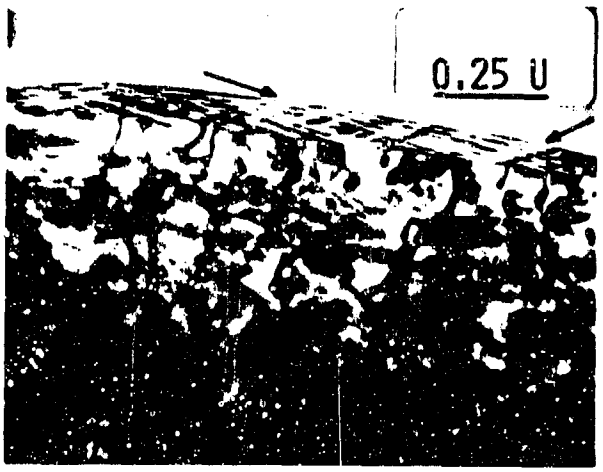

Fig. 12. Transmission electron micrograph of a 7475 Al alloy deformed at, a strain-rate of 10^{-4} s^{-1} and temperature of 457°C to a strain-level of 1.0, showing emission of dislocations from grain-boundary region. The arrows indicate two types of extrinsic grain-boundary dislocations.

Fig. 13. Transmission electron micrograph of a 7475 Al alloy deformed to strain of 1.0, at a strain-rate of 10^{-4} s^{-1} and temperature of 457°C, depicting interaction of dislocations with particles within the grain.

SECTION 5

SUPERPLASTIC DEFORMATION AND CAVITATION PHENOMENON IN 7475-ALUMINUM ALLOY

M. K. Rao, J. E. Franklin and A. K. Mukherjee

ABSTRACT

The rate parameters for the constitutive expression for superplasticity in 7475-T6 aluminum alloy are determined from the analysis of mechanical data. The cavitation phenomenon in this industrially significant alloy is studied and the effect of hydrostatic gas pressure in minimizing the incidence of cavitation is demonstrated.

INTRODUTION

Fine grained 7475-T6 aluminum alloy has substantial potential for superplastic forming operations [1-3]. It is now possible to produce such fine grain microstructure by thermomechanical processing [2]. The key element in such a processing step is the ability of the Cr-rich intermetallic particles to pin the grain boundaries. The present work was undertaken in order to obtain the rate parameters to elucidate the deformation mechanism for superplasticity in this alloy. A second point of emphasis was to study the cavitation phenomenon. This alloy cavitates easily during superplastic deformation, primarily by decohesion of the particle/grain boundary interface. The application of hydrostatic gas pressure during concurrent superplastic deformation was shown to substantially reduce the incidence of cavitation.

The experimental results were analyzed using the Mukherjee-Bird-Dorn [4] relation for elevated temperature plasticity.

$$(\dot{\varepsilon}kT)/(DGb) = A(b/d)^p (\sigma/G)^n \qquad (1)$$

where $\dot{\varepsilon}$ is the strain rate, the diffusivity $D = D_0 \exp(-Q/RT)$ and Q is the activation energy, G = shear modulus, σ = stress, d = grain size, p = grain size exponent, n = stress sensitivity parameter = 1/m where m is the strain rate sensitivity, A is a mechanism and structure dependent constant and KT has the usual meaning. The experimentally determined values of n, p, Q and A can assist in identifying the rate controlling deformation mechanisms.

EXPERIMENTAL PROCEDURE AND RESULTS

The 7475-T 6 alloy has an average grain size of 9 μm. The grain size was measured by taking the cube-root of the product of grain sizes in three mutually perpendicular directions. Grain sizes between 10 and 35 μm were obtained by statically annealing the specimens at 530°C for various lengths of time. Mechanical tests were conducted in an argon atmosphere using a computer-interfaced MTS machine and a constant strain rate test program. The tests were performed primarily at 457°C at strain rates of 10^{-5} to 5 x 10^{-3} per sec to a maximum true strain level of 1.4. The cavitation experiments were conducted in an Instron machine at constant crosshead speed using a specially designed apparatus that enabled us to maintain a hydrostatic pressure of argon gas during the tensile tests.

Mechanical Properties

The true stress-true strain curves were used to obtain the double logarithmic plot of the true stress vs strain rate at various strain levels as shown in Fig. 1. The curves show the typical sigmoidal shape. At low strain rate range there is clear evidence of strain hardening. The tendency for this behavior decreases with increase in strain rate. The values for strain rate sensitivity parameter, $m = (\partial \log\sigma / \partial \log\dot{\varepsilon})$ was determined at various strain level from the slope of the $\log\sigma$ vs $\log\dot{\varepsilon}$ curves. The grain size sensitivity parameter parameter, p was determined from the slope of double logarithmic plot of stress vs initial grain size at various strain levels. The activation energy for superplastic flow in the temperature range 437 to 517°C was obtained from a plot of $\log(\sigma^{-n} G^{n-1} T)$ versus 1/T as shown in Fig. 2. The average value of the activation energy Q is 162 KJ/mole and it was not a function of strain or grain size. The structure parameter A was obtained from a normalized plot of $[(\dot{\varepsilon}kT)/(DGb)](d/b)^p$ versus σ/G. The A-values at various strains were obtained by extrapolating the straight line plots for different strain levels to intersect the y-axis at $\sigma/G = 10^{\circ}$. The estimated A-value decreases as the imposed strain level is increased. The results for these rate parameters are summarized in Table 1.

TABLE 1 The Variation of Rate Parameters with Superplastic Strain

Parameter	ϵ=0.5	ϵ=0.7	ϵ=1.0
m	0.549	0.531	0.520
n	1.82	1.88	1.92
p	2.16	1.56	1.30
Q(KJ/mole)	146	173	166
A	5.30×10^6	9.3×10^3	2.2×10^2

Cavitation Aspects

Preliminary studies indicated that the constituent particles present in this alloy are intimately involved in the nucleation of cavities during superplastic deformation. TEM investigation revealed grain boundary cavities at an early strain associated with such particles. The extent of cavitation was definitely a function of strain. The effect of hydrostatic gas pressure on the stress-strain curves was dramatic. One observed significant increase in terminal ductility at 200 to 600 psi gas pressure over atmospheric condition and yet bigger increase at 800 psi gas pressure. This increase in terminal ductility is demonstrated in Fig. 3. Using 800 psi confining pressure and an engineering strain rate of 6.7 x 10^{-4} s^{-1} at 457°C, the specimen did not fail even at 1330 percent engineering strain. A pictorial depiction of specimen elongation at various level of confining gas pressure is shown in Fig. 4.

DISCUSSION AND CONCLUSIONS

The values of the rate parameters shown in Table 1 are in agreement with the general trend and predictions of the common models for superplasticity. The stress sensitivity has a value close to two which is the usual prediction of models. The measured activation energy (162 KJ/mole) for superplasticity is close to that for lattice diffusion [5] in pure aluminum, i.e., 142 KJ/mole. The value of the grain size exponent p is approximately equal to two but it decreases with increase in strain. It is likely that this change in the value for p is associated with change in grain shape, i.e., some extent of grain elongation during superplastic flow. Optical microscopy revealed that under all testing condition, negligible changes in the grain size occurred although deformation induced grain elongation did take place to some extent. The discrepancy between this observation and that of Hamilton et al. [3] may be due to the fact that this was a different "heat", i.e., type B category of ingot. Additionally, it maybe due to the fact that in the present work grain size was quoted after making measurement in three mutually perpendicular directions. The decrease in the estimated value of the parameter A with increasing strain is very likely associated with increase in dislocation density as well as with changes in the value of grain size sensitivity parameter with strain. TEM studies clearly revealed increased dislocation density with increase in superplastic strain and significant level of dislocation-particle interaction. The activation energy for

superplasticity was closer to that for volume diffusion. In Al-Zn eutectoid, which does not contain any precipitates, the activation energy for superplasticity is equal to that for grain boundary diffusion. It may be that in this alloy the dislocation has to climb over the blocking intermetallic particles in the grain interior before they can arrive at their annhilation sites, possibly at grain boundaries. In a sequential event, the slower step, i.e., the lattice diffusion controlled climb of the dislocations over the particles will control the rate. This may explain the higher value for the activation energy for superplasticity that is observed here. A recent investigation by Belzunce, Reese and Sherby [6] on the same alloy suggests the possibility of two independent creep contributions. These are, grain boundary sliding accomodated by slip, representing "mantle" deformation and slip creep presenting "core" deformation. Our electron microscopic observation is in agreement with the above suggestion.

Both optical microscopy and TEM study revealed a process of interlikage of cavities at atmospheric pressure as a function of strain. The cavities link up and elongate along the direction of tensile axis. This suggests that the cavities probably grow by continuum hole growth process [8]. The superplastic ductility in this alloy is obviously increased [7] very substantially by superimposing argon gas pressure. The most remarkable aspect of this extraordinary ductility is the fact that it has been achieved by virtually eliminating internal grain boundary cavitation and hence internal necking. The ongoing investigation will now try to ascertain if the effect of superimposed pressure is to reduce the rate of nucleation of cavities, the rate of growth of cavities or both. It will also address the question whether the decrease in or sometimes the lack of cavitation is because they just got sintered away or if they are simply being crushed by the imposed pressure and only appear to be eliminated. Such questions need be answered before the beneficial effect of hydrostatic pressure on cavitation can be fully assessed.

ACKNOWLEDGEMENTS

This work was supported by the Air Force Office for Scientific Research.

REFERENCES

1. J. A. Wert, N. E. Paton, C. H. Hamilton and M. W. Mahoney, Met. Trans., 12A, 1265 (1981).
2. N. E. Paton, J. A. Wert, C. H. Hamilton and M. W. Mahoney, J. of Metals, 34, 21 (1982).
3. C. H. Hamilton, C. C. Bampton and N. E. Paton in Superplastic Forming of Structural Alloys, (edited by N. E. Paton and C. H. Hamilton), P. 173, TMS-AIME, Warrendale, PA (1982).
4. A. K. Mukherjee, Annual Reviews of Materials Science, 9, 191 (1979).
5. T. S. Lundy and J. F. Murdock, J. Appl. Phy., 33, 1671 (1962).
6. J. M. Belzunce, K. Reese and O. D. Sherby, to be published.
7. C. C. Bampton, M. W. Mahoney, C. H. Hamilton, A. K. Ghosh and R. Raj., Met. Trans., 14A, 1583 (1983).
8. J. W. Hancock, Met. Sci., 10, 319 (1976).

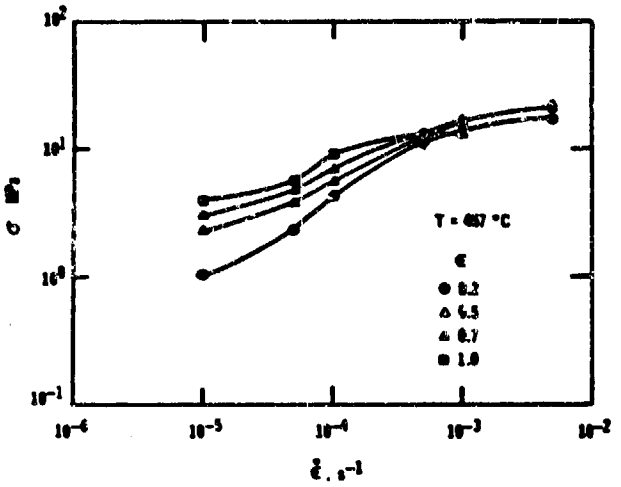

Fig. 1. True stress vs true strain rate behavior.

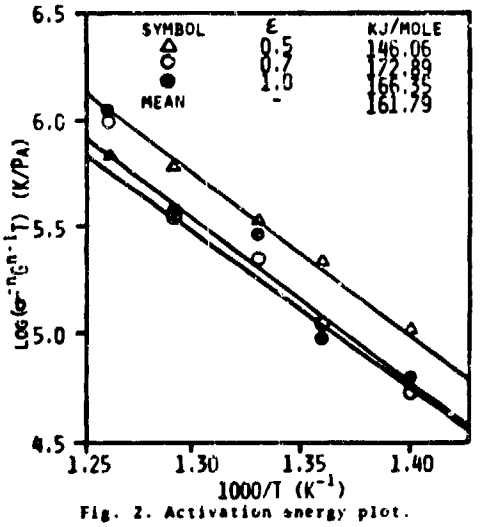

Fig. 2. Activation energy plot.

Fig. 2. Activation energy plot for various strains.

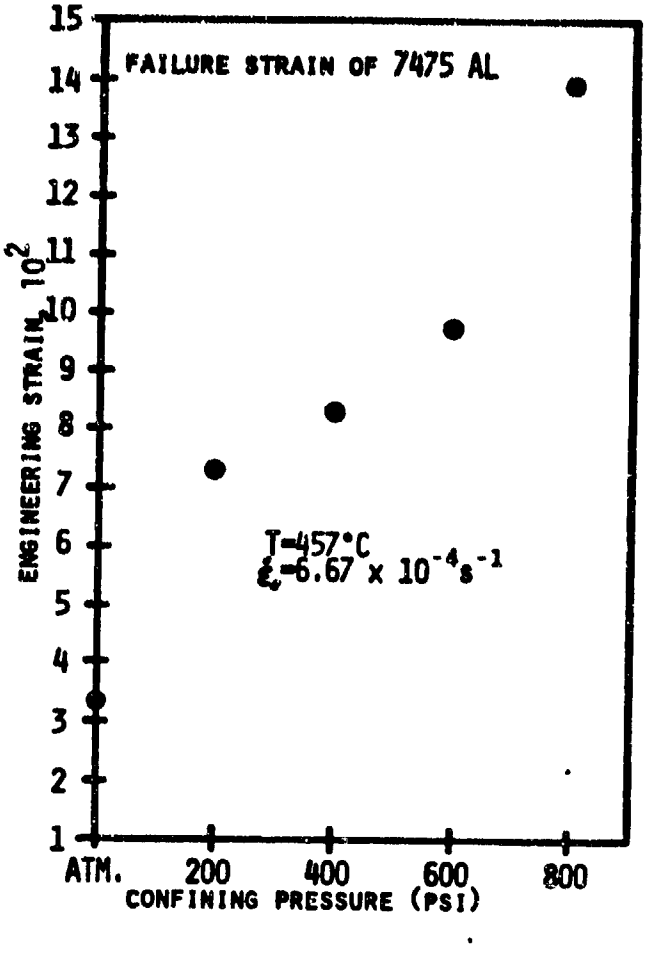

Fig. 3. Engineering failure strain vs confining pressure.

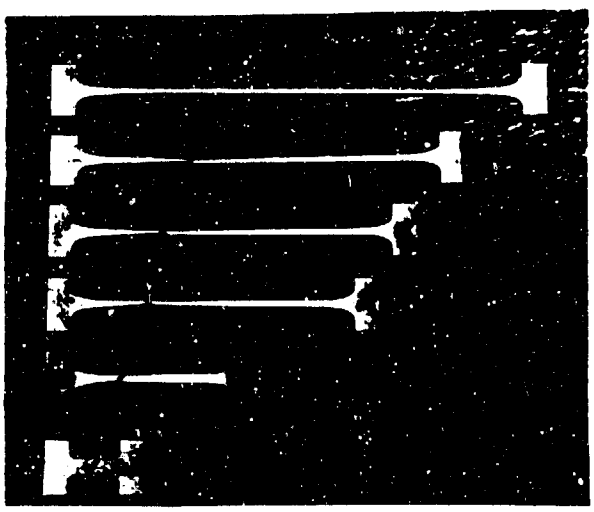

Fig. 4. 7475 Al failure strain at various pressures. (top to bottom) p=800 psi, 1330 w/o failure; p=600 psi, 980 ; P=400 psi, 830 ; P=200 psi, 720 ; P=atm, 330 ; undeformed sample. ($T=457^{\circ}C$, $\dot{\epsilon}_E=6.67\times10^{-4}s^{-1}$)

SECTION 6

List of Publications from AFOSR Support

A-In Print

1980 1. LOW STRESS AND SUPERPLASTIC CREEP BEHAVIOR OF Zn-22% Al EUTECTOID ALLOY,
A. Arieli, A. K. S. Yu, and A. K. Mukherjee, Metallurgical Transactions, Vol. 11A, pp. 181-191.

2. FACTORS AFFECTING THE MAXIMUM ATTAINABLE DUCTILITY IN A SUPERPLASTIC TITANIUM ALLOY,
A. Arieli and A. Mukherjee Materials Science and Engineering, Vol. 43, pp. 47-54.

3. HIGH-TEMPERATURE DIFFUSION-CONTROLLED CREEP BEHAVIOR OF THE Zn-22% Al EUTECTOID TESTED IN TORSION,
A. Arieli and A. K. Mukhjerjee, Acta Metallurgica, Vol. 10, pp. 1571-1581.

1981 4. AN EVALUATION OF THE EFFECTS OF CONCURRENT GRAIN GROWTH DURING SUPERPLASTIC FLOW OF THE Ti-6Al-4V ALLOY,
A. Arieli, B. J. MacLean and A. K. Mukherjee, Proc.of the 4th Intnl. Conf.on Titanium, Kyoto, Japan, Ed. H. Kimura and O. Izumi, pp. 1047-1056.

5. TWO- AND THREE-DIMENSIONAL DEFORMATION MECHANISM MAPS FOR HIGH TEMPERATURE CREEP OF Zn-22% Al EUTECTOID ALLOY,
A. Arieli and A. K. Mukherjee, Materials Science and Engineering, Vol. 47, pp. 113-120.

6. REPLY TO "A CRITICAL EVALUATION OF THE CONCEPT OF A UNIVERSAL PARAMETER TO UNIQUELY SPECIFY HIGH TEMPERATURE CREEP MECHANISMS",
A. Arieli and A. K. Mukherjee, Scripta Metallurgica, Vol. 15, Sept. 81, p. 1053.

1983 7. THE EFFECT OF STRAIN AND CONCURRENT GRAIN GROWTH ON THE SUPERPLASTIC BEHAVIOR OF THE Ti-6Al-4V ALLOY,
A. Arieli, B. J. McLean and A. K. Mukherjee, Res Mechanica, Vol. 6, pp. 131-159, 1983.

8. ELEVATED TEMPERATURE CAVITATION IN CREEP AND SUPERPLASTICITY OF Ti-6Al-4V ALLOY,
G. Gurewitz, N. Ridley and A. K. Mukherjee, Proceedings of the International Conference on Fracture Mechanics, Nov. 1983, Published by the Chinese Society of Theoretical and Applied Mechanics, p. 898, Science Press, Beijing, China, 1983.

1984 9. MECHANICAL AND MICROSTRUCTURAL ASPECTS FOR OPTIMIZING THE SUPERPLASTIC DEFORMATION OF Ti-6Al-4V ALLOY B. Hidalgo-Prada, G. Gurewitz and A. K. Mukherjee, Proceedings, Intn' Amer. Conf. on Mat. Tech., San Juan, Puerto Rico, Ed, D. Black, p.18-1, 1984.

10. A METALLOGRAPHIC STUDY OF CAVITATION IN Ti-6Al-4V ALLOY,
G. Gurewitz and A. K. Mukherjee, Advances in Fracture Research, Ed., S. R. Valluri, et al., Pergamon Press, Oxford, p. 2319-2324, 1984.

1985 11. CREEP AND DISLOCATION SUBSTRUCTURE,
L. Bondersky, A. Rosen and A. K. Mukherjee, Invited Review, International Metals Review, Vol. 30, p. 1, 1985.

12. ON THE NEW MODELS OF SUPERPLASTIC DEFORMATION
B. P. Kashyap and A. K. Mukherjee, Proceeding of International Conference on Superplasticity, Grenoble, France, pp. 4.1-4.31, Sept. 1985.

13. MICROSTRUCTURAL EVOLUTION DURING SUPERPLASTIC DEFORMATION IN A Ni-MODIFIED Ti-6Al-4V ALLOY.
B. Hidalgo-Prada and A. K. Mukherjee, Scripta Metallurgica, Vol. 19, pp. 1235-1239, 1985.(No acknow. on manuscript)

14. THE STRAIN RATE SENSITIVITY VALUES IN SUPERPLASTIC DEFORMATION
G. Gurewitz and A. K. Mukherjee, Materials Science and Engineering, Vol. 70, p. 191-196, 1985.

B-1 IN PRESS

1. CORRELATION BETWEEN MECHANICAL PROPERTIES AND MICROSTRUCTURE IN A NI-MODIFIED SUPERPLASTIC Ti-6Al-4V ALLOY.
B. Hidalgo-Prada and A. K. Mukherjee, Proceedings of ICSMA-7, Montreal Canada.

2. SUPERPLASTICITY-CORRELATION BETWEEN STRUCTURE AND PROPERTIES
M. Suery and A. K. Mukherjee, Creep Behavior of Crystalline Solids, ed. B. Wilshire, Pineridge Series on Progress in Creep and Fracture, Pineridge Press, Swansea G.B., 1985.

3. REVIEW: CAVITATION BEHAVIOR DURING HIGH TEMPERATURE DEFORMATION OF MICROGRAINED SUPERPLASTIC MATERIALS
B. P. Kashyap and A. K. Mukherjee, Invited review, to be published in Res Mechanica.

B-3 IN PREPARATION

1. EVIDENCE OF VISCOUS CREEP IN ALPHA-BRASS
B. Hidalgo-Prada and A. K. Mukherjee, Materials Science and Engineering.

2. INCREMENTAL-DECREMENTAL TESTS
G. Gurewitz and A. K. Mukherjee, Material Science and Engineering.

3. STRUCTURAL/MECHANICAL RELATIONS IN Ti-6AL-4V
G. Gurewitz and A. K. Mukherjee, Scripta Met.

4. CAVITATION NUCLEATION DURING THE CREEP OF ALPHA-BRASS
B. Hidalgo-prada and A. K. Mukherjee, Acta Metallurgica.

5. CAVITY NUCLEATION IN 7475 AL ALLOY
M. K. Rao and A. K. Mukherjee, Scripta Met.

SECTION 7

LIST OF PERSONNEL INVOLVED IN THE RESEARCH

1.	A. K. Mukherjee	Professor of Materials Science, Division of Materials Science and Engineering, Department of Mechanical Engineering, University of California, Davis, CA 95616
2.	M. Meier	Research Assistant, Department of Mechanical Engineering, University of California, Davis, CA 95616
3.	M. K. Rao	Formerly Research Assistant, University of California, Davis, now at Northwestern University, Evanston, Illinois
4.	J. E. Franklin	Unsupported Graduate Research Student, University of California, Davis, CA 95616, formerly Teaching Assistant
5.	B. Hidalgo-Prada	Formerly Research Assistant at University of California, Davis, CA 95616, now at the University of Venezuela at Cumana, Venezuela

SECTION 8

LIST OF COUPLING ACTIVITIES WITH OTHER GROUPS

a) Dr. Amit Ghosh
North American Science Center
Thousand Oaks, CA 91360

b) Dr. Jeffery Wadsworth
Lockheed Palo Alto Research Laboratory
Palo Alto, CA 94304

c) Dr. Adi Arieli
Mantech Fabrication Group
Airplane Division
Northrop Corporation
Hawthorne, CA 90250